August, 2010

PhD Dissertation

Numerical reconstruction of digital holograms and its application to three-dimensional imaging

Naseem Akhter

Department of Mechanical Design Engineering
Graduate School of Chosun University,
Gwangju, Republic of Korea

Numerical reconstruction of digital holograms and its application to three-dimensional imaging

August 25, 2010

by

Naseem Akhter

Department of Mechanical Design Engineering

Graduate School of Chosun University

Numerical reconstruction of digital holograms and its application to three-dimensional imaging

Approved by
Kyeong-Suk Kim, Ph.D.
Major Advisor

A dissertation submitted in partial fulfillment of the requirements for the degree of Doctor of Philosophy

April, 2010

Naseem Akhter
Department of Mechanical Design Engineering
Graduate School of Chosun University

This certifies that the dissertation of
Naseem Akhter is approved.

Chair of Committee	Chosun University	Wan-Shik Jang
Committee Member	Chosun University	Jae-Yeol Kim
Committee Member	Chonbuk Nat. University	Dong-Pyo Hong
Committee Member	Korean Research Institute of Standards and Science	Man-Yong Choi
Thesis Advisor	Chosun University	Kyeong-Suk Kim

June, 2010

Graduate School of Chosun University

- CONTENTS -

- List of Figures -

ABSTRACT

Numerical Reconstruction of digital holograms and its application to three-dimensional imaging

By Naseem Akhter
Advisor : Prof. Kyeong-Suk Kim
Dept. of Mechanical Design Engineering
Graduate School of Chosun University

Digital holography is a symbiosis of physical optics and digital computers. In fabricating computer-generated holograms, numerical data produced by a computer are converted into a physical hologram or an optical element intended for forming real optical beams. For the last several decades, holographic method has been widely used to measure three-dimensional aspects of samples qualitatively and quantitavely. Numerical reconstruction of holograms offers much more possibilities than conventional processing. However numerical reconstruction only to the image planes parallel to the hologram plane cannot be interesting.

In this thesis, theoretical analysis of reconstruction of digital holograms using digital holography is reviewed. Three main reconstruction methods, which are the most widely used are described and compared. Zero- order and one of the twin image components can

be removed by using a numerical bandpass filter. These problems are completely removed by using a phase shift-digital holography.

The reconstruction of digital holograms in a plane parallel to image plane using a holographic recording scheme with a spherical reference beam and its application to three-dimensional imaging are described. Basic experimental set- up used to record the holograms of small particles for sectional image reconstruction in plane parallel to image plane and its application to the three-dimensional imaging are discussed. Furthermore, the off-axis digital holographic geometry is presented for the reconstruction of the digital hologram of small particles in an arbitrarily tilted plane. A single hologram is sufficient to obtain a well focused clear image on the tilted plane. We can't obtain clear images of small particles in the case of plane tilted to the detector plane by ordinary reconstruction method because of the rotation of the hologram plane. Rotational transformation based on coordinate rotation in Fourier space makes it possible to reconstruct holographic images in any plane in the object space.

Non-destructive applications of laser holography, based on vibration characteristic analysis using double-pulsed Ruby laser with a pulse duration of 30 ns, is presented to locate the delamination in laminated composite palates containing various sizes of artificial defects located at the centre of the specimen. The main advantage of this technique over conventional electronic speckle pattern interferometry is the ability to carry out measurements even under harsh environmental conditions.

국문 요약문

디지털 홀로그램의 수치적 복원과 3차원 이미지에 대한 그 활용

Naseem Akhter
지도교수 : 김경석
기계설계공학과
조선대학교 대학원

디지털 홀로그래피는 물리광학과 디지털 컴퓨터의 공생이다. 컴퓨터로 생성한 홀로그램을 조작함에 있어서, 컴퓨터에 의해 만들어진 수치적 데이터는 물리적인 홀로그램이나 실제 광학 빔을 형성하기 위해 의도된 광학 요소로 전환된다. 최근 수 십년간 홀로그래피 방법은 샘플의 3차원 형상을 정성적, 정량적으로 측정하기 위해 폭넓게 사용되어 왔다. 홀로그램의 수치적 복원은 기존의 처리과정에 비해 더 많은 가능성을 제공한다. 그러나 오직 홀로그램 평면에 평행한 이미지 평면에 대한 수치적인 복원만이 관심을 받을 수는 없다.

본 논문에서는, 디지털 홀로그래피를 이용한 디지털 홀로그램 복원의 이론적 해석이 검토된다. 가장 폭넓게 사용되는 3가지 주요 복원 방법이 기술되고 비교된다. 0차(Zero-order)와 이중 이미지 요소 중 한 개가 수치적인 대역통과 필터를 사용함으로써 제거된다. 또한, 위상이동 디지털 홀로그래피가 이중 이미지 문제를 극복하기 위해 사용된다.

구면 기준파와 함께 홀로그래피 저장 방식을 이용한 이미지 평면에 평행한 평면에서의 디지털 홀로그램의 복원과 3차원 이미지에 대한 활용이 기술된다. 이미지 평면에 평행한 평면에서의 부분적 이미지 복원을 위해 작은 조각의 홀로그램을 저장하는데 사용된 기본 실험장치와 3차원 이미지에 대한 그 활용이 논의된다. 더 나아가, 임의로 경사를 준 평면에서의 작은 조각에 대한 디지털 홀로그램의 복원과 3차원 이미지에 대한 그 활용도 논의된다.

시험편의 중앙에 위치한 다양한 크기의 인공 결함이 있는 복합재 적층판의 박리 위치를 찾기 위해 30 ns 펄스 지연을 갖는 이중 펄스 루비 레이저를 사용한 진동특성 해석에 기초한 레이저 홀로그래피의 비파괴적 활용이 제시된다. 기존의 ESPI(전자처리 스페클 간섭법)에 대한 이 기술의 주된 장점은 열악한 환경 조건하에서도 측정할 수 있는 능력이 있다는 점이다.

1. Introduction

Holography involves recording a modulated form of a desired (object) wave. It is also known as wave front reconstruction. The resulting device is called hologram. Digital holography is more commonly known as diffractive optics. Some other terminologies used for diffractive optics are computer-generated holography, diffractive optical elements and binary optics.

We are aware that a conventional photograph is a two-dimensional version of a three-dimensional scene. All the light originating from a single point of the scene and collected by the lens is focused to a single conjugate point on the image. By contrast, a digital hologram is made, as we shall see, without use of a lens or any other focusing device. The digital hologram is a complex inference pattern of microscopically spaced fringes, not an image of the scene. The real-life qualities of the image provided by the digital hologram from the preservation of information relating to the phase of the wavefront in addition to its amplitude or irradiance. To record these phase relationship as well, it is necessary to convert phase information into amplitude information. If the wavefront of light from the scene is made to interfere with a coherent reference wavefront, then the resultant interference pattern includes information regarding the phase relationships of each part of the wavefront with the reference wave and, therefore, with every other part.

Holography was first discovered by Dennis Gabor in 1948, which is before the invention of the laser [1.1]. He recognized that the intensity resulting from the sum of an object wave and a reference wave carries the information on both the amplitude and phase of the object wave. After the

invention of the laser as a coherent source, Gabor's ideas became a practical reality. Gabor illuminated the hologram in his original set-up by parallel beam through the mostly transparent object. Therefore the axes of both the object wave and the reference wave were parallel. The reconstruction of this hologram results in the real image superimposed by virtual image (twin-image) and zero order of diffraction (undiffracted wave). This set-up is commonly known as In-Line digital holography. Leith and Upatnieks were made significant improvements in In-Line holography, who introduced an off-axis reference wave. Their set-up separates the two images and the reconstruction wave spatially, that is known as Off-axis digital holography [1.2].

Zero-order diffraction and twin-images are the measure problems in digital holography. These problems are completely removed by using a phase shift-digital holography[1.3,1.4]. In off -axis holograms, the zero-order diffraction and the twin-images are distinct, image reconstruction is possible but the zero order and twin image are not separable in an In-Line set-up. However, for many reasons applications of an in-line set-up is advantageous than off-axis set-up. Several articles have been published in the literature that has successfully attempted to suppress the zero-order of diffraction and the twin image [1.5-1.8].

In this thesis, Zero- order and one of the twin image components has been removed by using a numerical band-pass filter. In this method the zero-order of diffraction and the twin image can be digitally eliminated by means of filtering to the corresponding pixels in the computed Fourier transform of the hologram.

Numerical reconstruction of hologram was initiated by Goodman and Lawrence [1.9] and by Yaroslavskii, Merzlyakov and Kronrod [1.10]. A big step forward was the development of direct recording of Fresnel holograms with charge coupled devices (CCD) by Schnars and Juptner[1.11]. This method enables now full digital recording and processing of holograms, without any photographic recording as intermediate step. Numerical reconstruction of digital holograms offers much more possibilities than conventional processing. Another advantage is that focusing can be adjusted numerically to reconstruct images at arbitrary positions after unfocussed holograms are acquired. To explore potential metrological applications of digital holography in micro-measurements and the requirement of high resolution as well as accuracy are the two major challenges. Also, in connection with the various methods for the 3D measurements, many reconstruction algorithms have been developed to meet the specific conditions and to add some useful capabilities.

For last several decades, holographic method has been widely used to measure 3D aspects of samples qualitatively and quantitavely. Digital holography is an active research topic for both macroscopic and microscopic three dimensional imaging such as surface profile, refractive index, 3D particle tracking etc. MEMS have let digital holography to gain more popularity as an effective mean of 3D microscopy.

This thesis is divided in two parts. First, the thesis focuses on the reconstruction of digital holograms in a plane parallel and as well as tilted to image plane using a lens-less holographic recording scheme with a spherical reference beam and its application to three-dimensional imaging.

Rest part deals with non-destructive applications of laser holography. The details structure of the thesis is as following. In first two sections, introduction and the futures of digital holography are discussed briefly. These sections describe the theoretical analysis, principle of digital holography, outlines the three numerical reconstruction methods and experimental set-ups of digital holography.

In Section3, the details of the experimental set- up is presented to record the holograms for micro-structure measurement, sectional image reconstruction and three-dimensional microscopy of small particles and a biological specimen, in plane parallel to image plane. Section4 describes the reconstruction of digital holograms for small particles in arbitrarily tilted plane and its application to three-dimensional imaging. Non-destructive applications of laser holography, based on vibration characteristic analysis using double-pulsed Ruby laser with a pulse duration of 30 ns, is described in section5, to locate the delamination in laminated composite palates containing various sizes of artificial defects located at the centre of the specimen and the last section concludes the thesis.

2. Theoretical Analysis

In this section, principle and theoretical analysis of digital holography are briefly reviewed. Geometrical configurations of some experimental set-ups are shown and typical features of them are discussed. The main reconstruction methods are described, which are most widely used in digital holography and compared each other.

2.1. Digital holography

In digital holography, holograms are recorded by a CCD camera and image reconstruction is performed by computer, thus saving the trouble of photographic processing. The optical system is also simple because we need no imaging lens. The concept of digital hologram recording is illustrated in Fig-2.1. A plane wave refracted from the object and a reference wave are interfering at the surface of the CCD camera. The resulting hologram is electrically recorded and stored in the computer memory [2.1-2.6]. In general, the object is a three dimensional body with diffusively reflecting surface, located at a distance d from the CCD. The holographic process is described mathematically using the following formalism. The complex amplitude of the object wave and reference wave are given by the following relations:

$$E_o(x,y) = a_o(x,y)e^{i\Phi_o(x,y)} \tag{2.1}$$

$$E_r(x,y) = a_r(x,y)e^{i\Phi_r(x,y)} \tag{2.2}$$

where Φ_o, Φ_r, a_o and a_r are the phase and real amplitude of the object wave and reference wave respectively. Both waves interfere at the surface of the recording medium of the CCD.

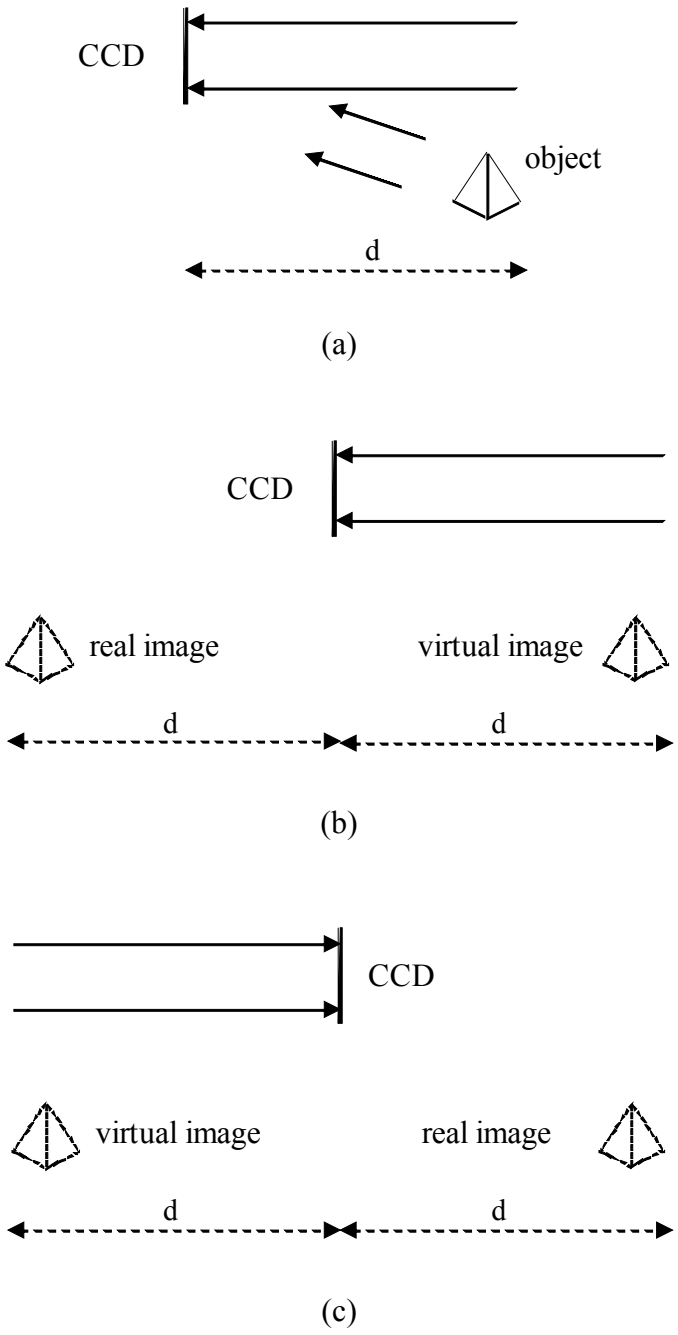

Fig.2.1 Digital holography (a)recording, (b)reconstruction with reference wave E_r and (c) reconstruction with conjugate reference wave E_r^*

The hologram function, which is proportional to the interfered intensity distribution on the recording medium, is calculated by,

$$h(x,y) = |E_o(x,y) + E_r(x,y)|^2 \\ = |E_o|^2 + |E_r|^2 + E_o E_r^* + E_o^* E_r \tag{2.3}$$

For holographic reconstruction, the hologram function has to be multiplied with the complex amplitude of the reconstruction (reference) wave.

$$E_r(x,y)h(x,y) = (|E_o|^2 + |E_r|^2)E_r + |E_r^*|^2 E_o + E_r^2 E_o^* \tag{2.4}$$

The first term on the right side of equation (2.4) corresponds to the undiffracted wave passing the hologram known as zero-order diffraction in optical reconstruction. The second term is the reconstructed object wave, forming the virtual image and the third term generates a distorted real image of the object. The virtual image appears at the position of the original object and real image is formed at a distance 'd' in the opposite direction to the CCD as shown in the Fig-2.1(b). The reason for the distortion of the real image is spatially varying complex factor E_o^2, which modulates the image forming conjugate object wave E_o^*. A non-distorted real image can be generated by using the conjugate reference beam E_r^* as shown in Fig-2.1(c):

$$E_r^*(x,y)h(x,y) = (|E_o|^2 + |E_r|^2)E_r^* + E_r^{*2} E_o + |E_r|^2 E_o^* \tag{2.5}$$

The wave fields in the equation (2.4) and (2.5) are not focused but diffracted ones. To reconstruct the wave-fields, they should be propagated optically or numerically to the image plane or the object plane apart from the hologram plane with the distance d as shown in the Fig-2.2.

The diffraction of a light wave at an aperture (in this case a hologram) which is mounted perpendicular to the incoming beam is described by Fresnel-Kirchhoff integral [2.2]

$$u(\alpha',\beta') = \frac{1}{i\lambda}\iint_{-\infty}^{\infty} E_r(x,y)h(x,y)\frac{1}{\rho'}e^{-i\frac{2\pi}{\lambda}\rho'}dxdy \tag{2.6}$$

where $\rho' = \left[(x-\alpha')^2+(y-\beta')^2+d^2\right]^{1/2}$ is the distance between a point in the hologram plane and a point in there constructed plane , λ is the wave length of the light wave, and $u(\alpha',\beta')$ is the reconstructed wave-field. The inclination factor is set to one, because the angles are approximately zero. For a plane reference wave $E_r(x,y)$ is simply given by the real amplitude:

$$E_r = a_r + i\,0 = a_r \tag{2.7}$$

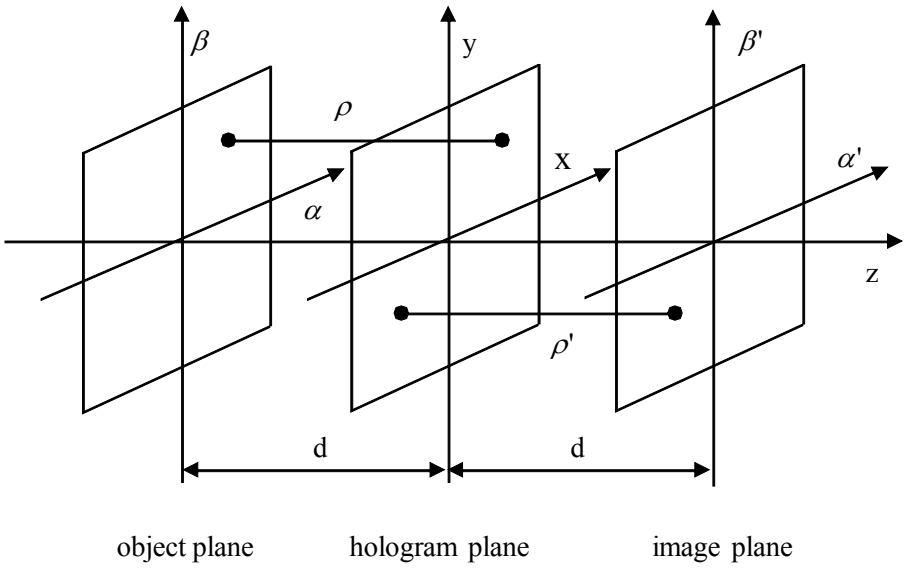

Fig.2.2 Coordinate system for numerical reconstruction

The diffraction pattern is calculated at a distance 'd' behind the CCD plane, which means it reconstruct the complex amplitude in the plane of real image. Equation (2.6) is the basis for numerical hologram reconstruction because the reconstructed wave field $u(\alpha',\beta')$ is a complex function, both the intensity as well as the phase can be calculated. This is in-contrast to the case of optical hologram reconstruction, in which only the intensity is made visible. This interesting property of digital holography is used in digital holographic interferometry.

From equation (2.4), we can see that the real image could be distorted. An undistorted real image can be produced by using the conjugate reference beam for the reconstruction as shown in equation (2.5). To reconstruct an undistorted real image in digital holography, therefore its necessary to insert E_r^* instead of E_r in the equation (2.6).

$$u(\alpha,\beta)=\frac{1}{i\lambda}\iint_{-\infty}^{\infty}h(x,y)E_r^*(x,y)\frac{1}{\rho}e^{-i\frac{2\pi}{\lambda}\rho}dxdy \tag{2.8}$$

where $\rho=\left[(x-\alpha)^2+(y-\beta)^2+d^2\right]^{1/2}$. This reconstruction scheme is shown in the Fig-2.1(c). The real image emerges at that position, where the object was located during recording. It should be mentioned that for the plane reference wave defined in equation(2.7) both reconstruction formulae, equations(2.6) and (2.8), are equivalent because $E_r=E_r^*\equiv a_r$.

2.2. Conventional photography versus digital holography

We are aware that a conventional photograph is a two-dimensional version of a three-dimensional scene, bringing into focus every part of the scene that falls within the depth of the lens. As a result the photography lacks the perception of depth or the parallax with which we view a real-life scene. In contrast, the digital holography provides a record of the scene that preserves these qualities. The hologram succeeds in effectively freezing and preserving for later observation the intricate wavefront of light that carries all the visual information of the scene. In viewing a hologram, this wavefront is reconstructed and we view what we would have seen if present at the original scene through the window define by the digital hologram. The reconstructed wavefront provides depth perception and parallax, allowing us to look around the edge of the object to see what is behind.

The real-life qualities of the image provided by the digital hologram from the preservation of information relating to the phase of the wavefront in addition to its amplitude or irradiance. Recording devices like ordinary photographic film and photomultipliers are sensitive only to the radiant energy received. When energy alone is recorded, the phase relationships of waves arriving from different directions and distances are lost. To record these phase relationship as well, it is necessary to convert phase information into amplitude information. The interference of light waves provides the requisite means. Recall that when waves interfere to produce a large amplitude, they must be in phase, and when the amplitude is minimum, the waves are out of phase, so that various contributions effectively cancel one another. If the wavefront of light from the scene is made to interfere with a

coherent reference wavefront, then the resultant interference pattern includes information regarding the phase relationships of each part of the wavefront with the reference wave and, therefore, with every other part. The situation is sometimes described by referring to the reference wave as a carrier wave that is modulated by the signal wave from the scene. This language provides a fruitful comparison with the techniques of radio wave communication.

In conventional photography a lens is used to focus the scene onto a film. All the light originating from a single point of the scene and collected by the lens is focused to a single conjugate point on the image. We can say that one-to-one relationship exits between object and image points. By contrast, a digital hologram is made, as we shall see, without use of a lens or any other focusing device. The digital hologram is a complex inference pattern of microscopically spaced fringes, not an image of the scene. Each paint of the digital hologram receives light from every pont of the scene or, to put it another way, every object point illuminated the entire hologram. There is no one-to-one correspondence between object points and points in the wavefront before reconstruction occurs. The digital hologram is a record of this wavefront.

2.3. Recording of digital holograms

In digital holography, holograms are recorded by CCD (charged coupled device) camera unlike conventional holography using holographic films. The small sensitive grains consist of holographic films, whose sizes are about 0.1 ~ 0.2 μm, make it possible to record very fine fringes of up

to 5000 lines per millimeter (L/mm) on the films. However, CCD's consist of a number of pixels with about 5 mm sizes can't resolve the fringes, whose densities exceed 100 L/mm. Therefore, more careful considerations are required for recording of digital holograms with CCD's. In the next section, spatial frequency requirements to resolve the interference patterns using CCD's are discussed.

2.4. Spatial frequency requirements

If arbitrary two plane waves enter on a screen with the incidence angle difference 'θ', the spatial frequency f of the fringes by the interference of the two can be easily obtained as follows:

$$f = \frac{2}{\lambda}\sin\frac{\theta}{2} \tag{2.9}$$

A CCD used to record holograms must resolve the interference pattern resulting from superposition of the reference wave with the waves scattered from the different object points. The maximum spatial frequency to be resolved is determined by the maximum angle $\theta_{\max}$ between these waves according to equation (2.1):

$$f_{\max} = \frac{2}{\lambda}\sin\frac{\theta_{\max}}{2} \tag{2.10}$$

Photographic emulsions used in optical holography have resolution up to 5000 L/mm. using these materials, holograms with angles of up to 180^{o} between the reference and the object waves can be recorded. However, the distance between neighboring pixels of a high resolution CCD is only in the order of $p \approx 5\mu m$. The corresponding maximum resolvable partial frequency

calculated by $f_{\max}=1/2p$ is therefore in the range of 100 L/mm. Combining this result and equation(2.2) leads to

$$f_{\max} = 2\sin^{-1}(\frac{\lambda}{4p}) \simeq \frac{\lambda}{2p} \tag{2.11}$$

where the approximation is valid for the small angles. The distance between neighboring pixels is therefore the quality, which limits the maximum angle between reference and object waves.

2.5. Reconstruction methods of digital holograms

Digital holograms, which are recorded on CCD's using off-axis or in line digital holography set-ups, are reconstructed by numerical procedures based on scalar diffraction theories. There are three main reconstructed algorithms most widely used. Each method has different properties with respect to available reconstruction distances, resolution of reconstructed images and computational load. It is very important to choose an appropriate method for the reliable reconstruction in a given situation.

2.5.1. Fresnel Transform Method (FTM)

Fresnel transform method (FTM) is most widely used and most popular one in digital holographic image reconstruction, because of its computational efficiency [1.10]. This method is based upon Fresnel diffraction formula expressed as follows:

$$u_z(x',y') = \frac{1}{i\lambda z}\exp[ik(z+\frac{x^2+y^2}{2z})]\iint u_o(x,y)\exp[ik(\frac{x^2+y^2}{2z})]\exp[-ik(\frac{x^2+y^2}{2z})]dxdy \tag{2.12}$$

The variables $u_o(x,y)$ and $u_z(x',y')$ are described in the Fig.2.3 mean the wave fields on the hologram plane and the image plane, respectively. Equation (2.12) can be solved by a single Fourier transform. Fast Fourier transform (FFT) algorithm makes the calculation of a hologram in a million data points completed in the order of ten milliseconds. The relation between the last exponent in equation.(2.12) and the FFT kernel leads to

$$\delta x' = \frac{\lambda}{N\delta x} \tag{2.13}$$

where $\delta x'$, δx and N are the pixel sizes of the image wavefield, holographic wavefield and the number of pixels, respectively. Therefore, the pixel size of the reconstructed image can vary according to 'z' and its value is just the same as the image resolution which can be achieved from numerical aperture (NA) of the digital holography system and the wavelength of the light source, i.e, $\delta x' = \lambda/2NA$.

Although Fresnel diffraction theory is valid for the whole Fresnel region, the applicability of this method is limited because the second exponent in equation (2.12), the parabolic phase factor, is changed in inverse proportion to reconstruction distance(z), it can't be made in a grid with a finite spacing without aliasing errors at large 'z' for the accurate reconstruction of digital holograms, therefore, the reconstruction distance requires the limitation of the following inequality:

$$z \geq \frac{L^2}{\lambda N} \tag{2.14}$$

where L is the side length of the hologram. In this region, Fresnel transform method makes the very fast reconstruction possible with the help of the built-in parabolic phase factor, resulting in real-time monitoring of samples [2.3].

2.5.2. Convolution method

The Fresnel diffraction formula can be also interpreted by a convolution approach accompanying with the rearrangement of the formula as follows [2.4]

$$u_z(x,y) = \frac{1}{i\lambda z}\exp(ikz)\iint u_o(x,y)\exp[ik(\frac{(x-x')^2+(y-y')^2}{2z})]dxdy \tag{2.14}$$

This equation has the form of a convolution integral. Therefore it can be expressed as the following simple expression:

$$u_z(x',y') = u_o(x',y') * p_z(x,y) = F^{-1}[U_o(\xi,\eta).P_z(\xi,\eta)] \tag{2.15}$$

asterisk and F^{-1} denotes the convolution operation and the inverse Fourier transform respectively where as $U_o(\xi,\eta)$ and $P_z(\xi,\eta)$ are the Fourier transforms of $u_o(x,y)$ and $p_z(x,y)$, respectively. Therefore, the scaling due to each transformation kernel, which is mentioned as the origin of the relation in equation (2.13), cancels out each other, that mean we can say, there constructed image has the same pixel size as the hologram. Instead of that, the pixel size of the frequency space $\delta\xi$ varies according to the following relation:

$$\delta\xi = \frac{\delta x'}{\lambda z} = \frac{\delta x}{\lambda z} \tag{2.16}$$

because the Fourier-transform space is another image plane in Fresnel transform method, but the frequency space in Convolution method. Also, the maximum frequency of the hologram or the reconstructed image becomes $N\delta/2\lambda z$. The limitation of the reconstruction distance 'z' is given by the maximum distance, at which $P_z(\xi,\eta)$ can be made without aliasing errors in an equispaced grid with the pixel-pitch $\delta\xi$:

$$z \le \frac{L^2}{\lambda N} \tag{2.17}$$

In convolution method, the limitation in equation (2.17) comes to be the upper bound rather than the lower bound as derived in equation (2.14) for the FTM. Both ranges overlap, permitting a calculation in the full range from the Fresenel diffraction region to the Fraunhoffer region, provided that the proper method is selected according to the distance.

2.5.3. Angular Spectrum Method (ASM)

The angular spectrum method (ASM), also known as plane wave expansion method, can accurately reconstruct the complex wave field on the image plane. The Geometrical configuration of the image and the hologram planes is shown in the Fig.2.3. The complex hologram and image wave fields $u_o(x,y)$ and $u_z(x',y')$ are considered to be the superposition of the plane waves with wave-vectors $k=(k_x,k_y,k_z)$ and $k'=(k_{x'},k_{y'},k_{z'})$. Suppose their Fourier transforms are

$$U_o(k_x,k_y)=\iint_{-\infty}^{+\infty}u_o(x,y)\exp[i(k_x.x+k_y.y)]dxdy \tag{2.18}$$

$$U_z(k_{x'},k_{y'})=\iint_{-\infty}^{+\infty}u_o(x',y')\exp[i(k_{x'}.x'+k_{y'}.y')]dx'dy' \tag{2.19}$$

If $k_x=k_{x'}$ and $k_y=k_{y'}$, the only difference between $U_o(k_x,k_y)$ and $U_z(k_{x'},k_{y'})$ is the transfer function '$P(k_z)$' where 'z' is the separation between the xy-plane and $x'y'$-planes.

$$U_z(k_{x'},k_{y'})=U_o(k_x,k_y)P(k_z) \tag{2.20}$$

$$\text{where } P(k_z)=\exp(ik_zz),\quad k_z=(k^2-k_x^2+k_y^2)\ \text{ and } k=2\pi/\lambda \tag{2.21}$$

Therefore, the reconstructed wave field $u_z(x',y')$can be obtained from the inverse Fourier transform of $U_z(k_{x'},k_{y'})$:

$$u_z(x',y')=F^{-1}[U_z(k_{x'},k_{y'})]=F^{-1}[U_o(k_x,k_y).P_z(k_z)] \tag{2.22}$$

Although the method based on Fresnel diffraction formula can still give an accurate reconstruction for smooth and slowly varying objects where the Fresnel approximation is not strictly satisfied, it can't correctly

reconstructed near wave-fields for more diffractive objects, where the higher-order terms in the expansion of the Fresnel approximation are more significant. Angular spectrum method can be a way out of those problems, because of its validity for the closer region that the Fresnel region [2.5-2.6].

ASM is a convolution-based method that uses FFT and IFFT successively as Convolution method does. Therefore, it has the same upper bound about 'z' as equation (2.17) and maintains the pixel size of reconstructed images. However this method can be used even for the closer region than the Fresnel region and is very useful for the measurement of microscopic samples requiring a high-NA imaging system as a necessity.

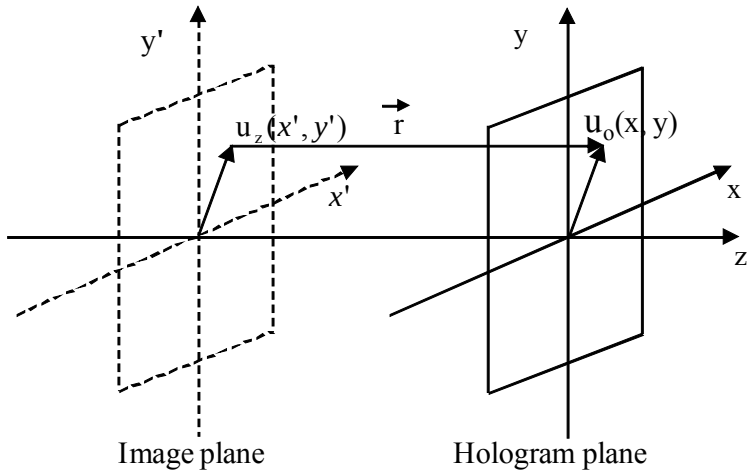

Fig.2.3 Geometrical configuration of the image and the hologram planes

2.6. Imaging analysis of digital holography

In this study we focus on understanding the system imaging mechanisms given rise to the unique characteristic of discretization in digital holography. Imaging analysis with respect to the system geometries is investigated and the corresponding requirements for reliable holographic imaging are specified. In addition, the imaging capacity of a digital holographic system is analyzed in terms of space-bandwidth product.

Image capacity means how much information is contained in measured signals and it can be explained by 'space-bandwidth-product' (SBP). It is defined as the number of pixels required for achieving maximal information capacity or the number of independent data points that are contained by the function in question [2.7-2.9]. If the SBP of a measured hologram is calculated, therefore it gives us the knowledge of the amount of information contained in the hologram. This quantity can be varied according to the set-ups in which the holograms are measured. In the case of conventional microscope, an object is imaged and its image is stored directly in a square CDD of pixel pitch 'p' and side length pN where N is the number of data points in the side length pN, the SBP of the image can be expressed as the multiplication of the spatial size 'Δx' and the frequency b and width (Δf) of the image:

$$\mathrm{SBP} = \Delta x \cdot \Delta f = A/p^2 = N^2 \tag{2.23}$$

where A is the area of the CCD. Therefore the image contains N^2 independent data points. The same implementation is possible in digital holography. The geometry configurations of In-line and Off-axis set-ups are depicted in Fig.2(a) and 2(b). In the case of In-line-digital holograms, the

maximum angular size of the (α) becomes approximately (λ/p), because the finest fringe spacing $(\lambda/\tan(\alpha/2))$ should be $2p$ to be recorded in the CCD without loss of frequency contents and them maximum frequency contained in the hologram is $(Np/2\lambda d)$. The frequency band width should be the double of the value, considering the negative frequencies. Thus, the SBP of the in-line digital hologram becomes

$$\begin{aligned} &\mathrm{SBP}_{\mathrm{in-line},x} = \alpha d(\Delta f) = N = \mathrm{SBP}_{\mathrm{in-line},y} \\ &\mathrm{SBP}_{\mathrm{in-line}} = \mathrm{SBP}_{\mathrm{in-line},x} \cdot \mathrm{SBP}_{\mathrm{in-line},y} = N^2 \end{aligned} \tag{2.24}$$

Therefore, in-line digital holograms can be made their SBP to be the same as the conventional microscope case. In the case of off-axis holograms the finest fringe spacing $(\lambda/\tan(\alpha+\theta_r))$ should be $2p$ and because of the asymmetry of the set-up, it must be also considered that the boldest fringe spacing $(\lambda/\tan(\theta_r-\beta))$ is infinite. These two relations lead to $(\alpha = \lambda/2p - \theta_r)$ and $\beta = \theta_r$, and the possible angular size of the object $(\alpha+\beta)$ is $\lambda/2p$. Furthermore, the frequency band width should be a half of that of the in-line case, because only a half portion of the frequency contents of the off-axis hologram is available, exclusive of the contents corresponding to the zero order diffraction and the conjugate wave field. Therefore the SBP of the off-axis digital hologram becomes as follows:

$$\begin{aligned} &\mathrm{SBP}_{\mathrm{off-axis},x} = (\alpha+\beta)d(\Delta f) = N/2 = \mathrm{SBP}_{\mathrm{off-axis},y} \\ &\mathrm{SBP}_{\mathrm{off-axis}} = \mathrm{SBP}_{\mathrm{off-axis},x} \cdot \mathrm{SBP}_{\mathrm{off-axis},y} = N^2/4 \end{aligned} \tag{2.25}$$

Therefore, in the case of off-axis digital holograms, the SBP becomes a quarter of N^2, even in the same CCD and the same arrangement of the imaging optics as those of the in-line case.

In conclusion, for the applications of digital holography, especially in the field of micro-measurement, studies on imaging performance are of particular importance. It is concluded from the analysis that, an in-line system can exhibit better performance, both in terms of a larger effective field of view and a higher imaging resolution.

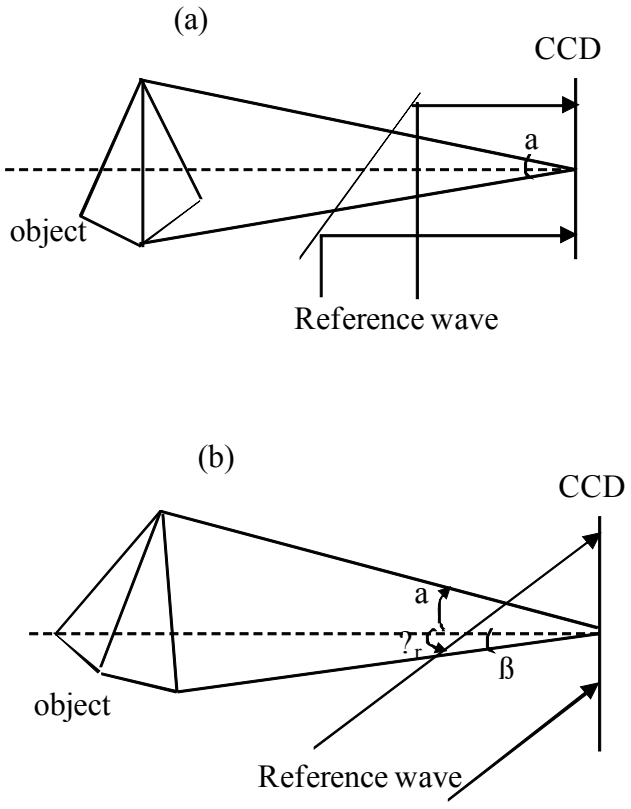

Fig.2.4 Geometrical configuration of beam (a) In-line (b) Off-axis

2.7. Zero-order of diffraction and twin image problem

Digital holography is an active research topic for both macroscopic and microscopic three dimensional imaging. It uses a charged-couple devices (CCD) camera for hologram recording and these digitalized holograms are reconstructed numerically. There are many methods of numerical image reconstruction in digital holography.

Zero-order diffraction and twin-images are the measure problems in digital holography. These problems are completely removed by using a phase shift-interferometry [1.3]. In off-axis holograms, the zero-order diffraction and the twin-images are distinct, image reconstruction is possible but the pixel sizes of the reconstructed hologram reduce to one fourth of the original even in the case of same CCD and the same arrangement of the optics as those of the in-line case [2.9]. The zero order and twin image are not separable in an In-Line set-up. However, for many reasons applications of an in-line set-up is advantageous than off-axis set-up. Several articles have been published in the literature that has successfully attempted to suppress the zero-order of diffraction and the twin image [1.4-1.7]. Etienne Cuche et al used spatial filtering for zero order and twin-image elimination. In this method the pixel sizes of the reconstructed hologram becomes a quarter of the original. H. Cho et al used intensity-averaging method to suppress zero order term [2.10].

Yamaguchi and Zhang [1.3] have presented phase-shifting digital holography in which four frames of in-line holograms and one frame of the intensity pattern of the object wave front were recorded. Similar phase-shifting approach was presented by Takaki et al [2.11], in which they

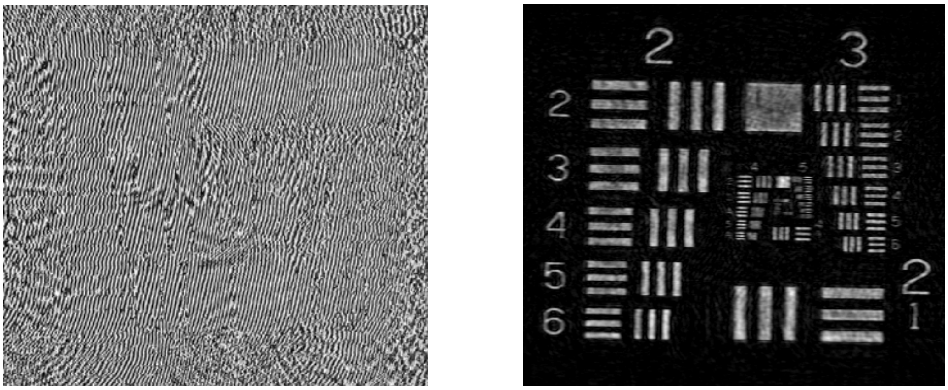

(a) (b)

Fig.2.5 (a) Phase-map image (b) Reconstructed image by phase-shifting digital holography

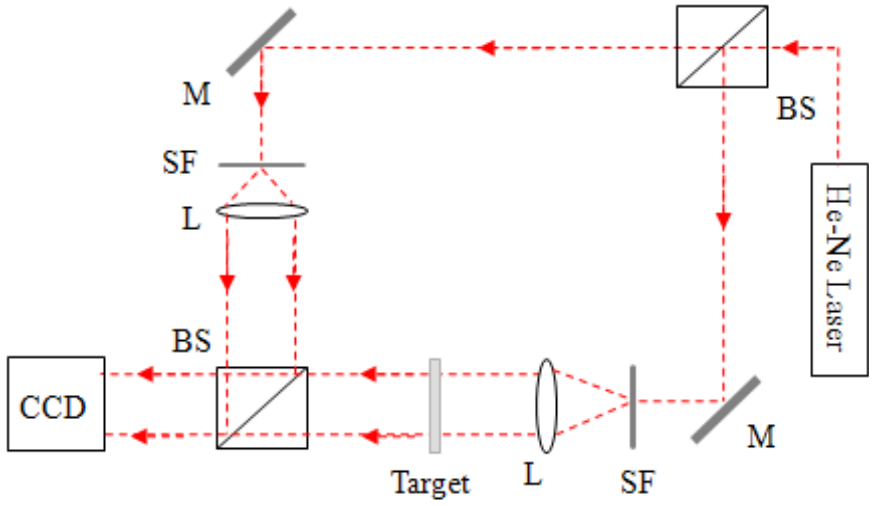

Fig.2.6 Set-up of the phase-shifting In-line digital holographic system. BS, beam splitter; M1, mirror with a PZT; M2, mirror; SF,spatial filter; L, collimating lens.

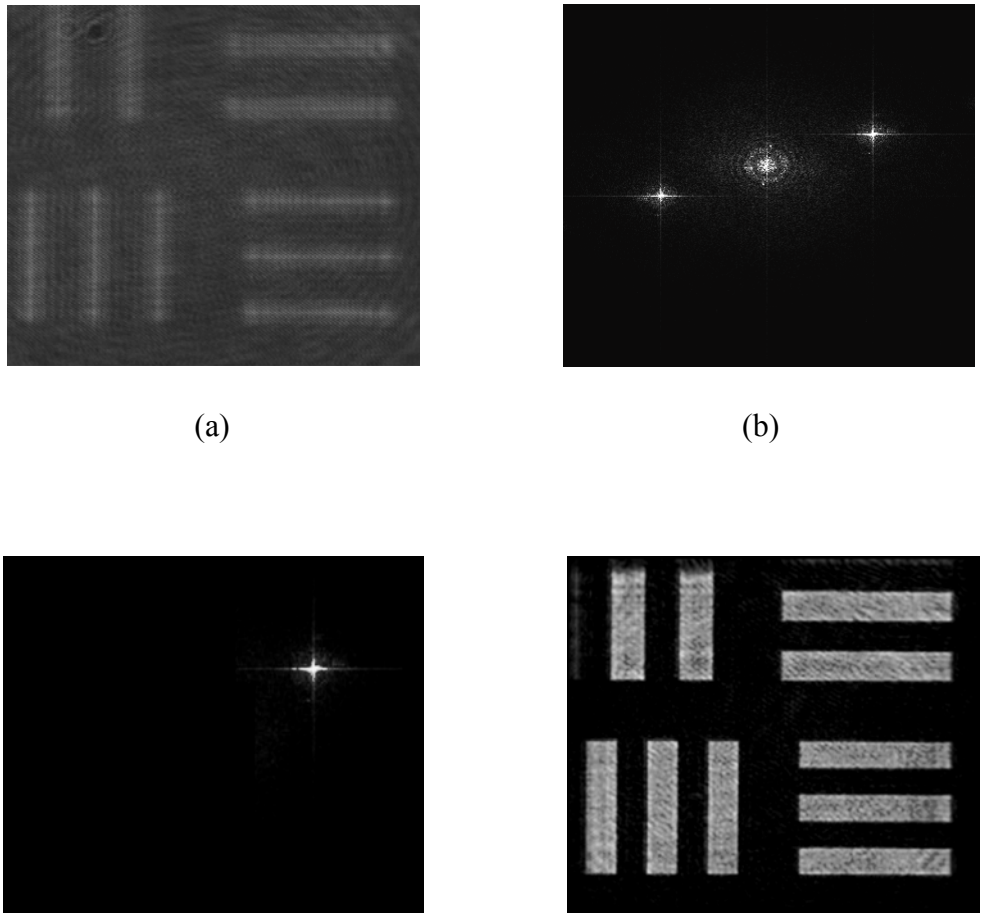

(a) (b)

(c) (d)

Fig.2.7. (a) Original hologram (b) Fourier spectrum of the hologram (c) Zero-order and twin-image removed hologram (d) Reconstructed image

only considered the off-axis holograms. For image reconstruction, the diffraction pattern on the CCD plane was obtained from the phase-shifted holograms with a phase-shifting method. The phase map image and reconstructed image from phase map are shown in the Fig.2.5. In our study, the superposition of the object wave and reference wave produces a holographic interference pattern that is recorded by CCD camera. Using angular spectrum method (ASM), one can extract information about wave field that give rise to the holographic interference pattern. Suppose that the hologram plane and the parallel image plane are designated by (x,y,z) and (x',y',z') coordinates, respectively. The two dimensional complex wave field on the parallel image plane, $u_z(x',y')$ is numerically reconstructed from the complex hologram wave field, $u_o(x,y)$ using angular spectrum method (ASM) that can accurately reconstruct the complex wave field on the image plane. The angular spectrum is the Fourier transform

$$F(k_x, k_y; 0) = \iint_{-\infty}^{+\infty} u_o(x,y)\exp[i(k_x.x + k_y.y)]dxdy \tag{2.26}$$

Where k_x and k_y are the spatial frequencies. Normally this spectrum contains zero-order diffraction and a pair of twin images components. The real image and virtual image are located symmetrically with respect to the centre of the image. Their distances to the centre depend on the incidence angle of the reference wave, which must be large enough to ensure a complete separation of the zero-order diffraction. Zero-order and one of the twin image components can be removed by using a numerical bandpass filter. The reconstructed wave field can be obtained from the inverse Fourier transform of the filtered angular spectrum.

$$u_z(x',y';z) = \iint_{-\infty}^{+\infty} F(k_x,k_y)\exp[i(k_x.x + k_y.y + k_z.z)]dk_x dk_y \qquad (2.27)$$
$$= F^{-1}[F(k_x,k_y;0).\exp(ik_z z)]$$

where $k_z = (k^2 - k_x^2 + k_y^2)$, $k = 2\pi/\lambda$ and $'z'$ is the separation between the image plane and hologram plane. The main advantages of the angular spectrum method are consistent pixel resolution, easy filtering of noise and background components, and the object to hologram distance can be any small distance without being limited by the minimum distance requirement. The computational procedure is not heavier in this case compared to the Fresnel approximation and other methods. The numerical diffraction of the hologram results in the reconstructed optical field as a matrix of complex numbers, yielding the amplitude and phase images. This method is intrinsically simple and does not require any additional apparatus. This method can yield a good significant improvement in the quality of reconstructed images.

An experiment is performed to demonstrate the theoretical analysis for phase-shift digital holography and the schematic set-up is shown in the Fig.2.6. In this digital holography experiment, a 1951 USAF resolution target was used and illuminated with a collimated He-Ne laser beam of wavelength 632.8 nm. The resolution target was located on the optical z-axis at a distance of 41.5 mm in-front of the CCD plane. The holograms formed by the interference between the object and the reference beams were captured by a CCD camera with the pixel size N x N = 960 × 1280 and pixel pitch 4.65 μm. The diffraction pattern on the CCD plane was obtained by Mech-Zender Interferometer and is shown in Fig.2.7 (a). The Fourier transform of the reconstructed wave field on the plane parallel to the CCD

plane is shown in the Fig.2.7(b). This image contains a real image, a virtual image, and a zero order of diffraction. The real image and virtual image are located symmetrically opposite with respect to the centre of the image. Their distances to the centre depend on the incidence angle of the reference wave, which must be large enough to ensure a complete separation of the zero-order diffraction. The separation of the real image and virtual image can be control by second beam splitter. The zero- order and one of the twin image components can be removed by using a numerical bandpass filter. For convenience, first of all the transformations were performed after padding the 960 × 1280 original wave field with zeros to make it a 1280 × 1280 square matrix, thus the pixel size in the k_x direction is the same as that in the k_y direction. The Fourier transform of the filtered angular spectrum is shown in the Fig.2.7(c). The reconstruction of digital hologram is based on the plane wave expansion method, it's also called angular spectrum method and reconstructed image is shown in Fig.2.7(d). The pixel sizes of there constructed hologram are same as the original hologram.

3. Micro-structure measurement and 3D imaging based on digital holography

We demonstrate micro-structure measurement, sectional image reconstruction and three-dimensional microscopy of small particles and a biological specimen in this section. We used holographic methods to obtain 2D and 3D images of small particles and a biological specimen. A single hologram is sufficient to obtain a section containing only the focused parts of the reconstructed image. One can obtain images of different plane sections of a specimen in addition to its 3D display. The reconstruction of a digital hologram is based on the plane-wave expansion of the diffracted wave fields using Fourier optics (this method is also known as the angular spectrum method). With this method, the object-to-hologram distance can be quite small because the minimum-distance requirement does not apply. Furthermore, numerical reconstruction of transparent objects by this method may be interesting for micro-structure measurement.

3.1. Introduction

Digital holography is an active research topic for both macroscopic and microscopic three dimensional imaging. Holographic three-dimensional (3D) displays provide realistic images without requiring special eyewear, which makes this technology a valuable tool for applications such as micro-measurements, medical imaging, industrial and military imaging [3.1,3.2]. For potential metrological applications of digital holography in micro-measurements, the requirements of high resolution as well as accuracy

are the two major challenges. It is thus important to choose the appropriate reconstruction method for better image quality and high accuracy. There are many methods of numerical image reconstruction in digital holography; the main ones are Fresnel transform method, Convolution method, and Angular spectrum method (ASM) are the main methods [3.3-3.5], in the order of long to short reconstruction distance. For the present work, we reconstruct a digital hologram by using the ASM, which is also known as the plane-wave expansion method. However, our main interest lies in three-dimensional holographic displays and sectional image reconstruction of digital holographic images.

Digital holographic microscopy has been demonstrated in many applications, including for observation of biological samples, living cells analysis, and velocimetry [3.6-3.8]. Several articles explain the three-dimensional microscopy using digital holography [3.9-3.11]. The aim of this publication is not to present a novel reconstruction method but to demonstrate that the selective numerical reconstruction method may be helpful in three-dimensional microscopic and tomographic imaging using digital holography. Another superiority of digital holography is that focusing can be adjusted numerically to reconstruct images at arbitrary positions after unfocused holograms are acquired.

We first present the method of reconstructing holograms, following which we present an example of particle field digital holography and its sectional image reconstruction. Furthermore, in reconstructing any given plane, the hologram can be viewed as containing defocused light and many spurious structures from the other sections. With this reconstruction method,

we can choose a section containing only the focused parts of the image. brief experimental procedure is explained in the following section.

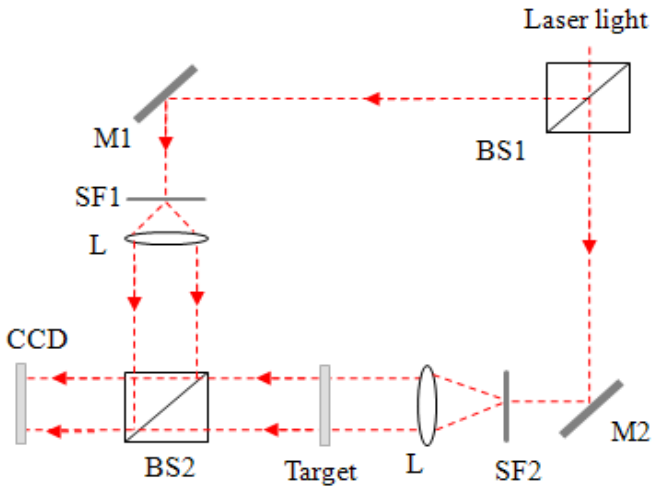

Fig.3.1.Geometrical of the experimental set-up

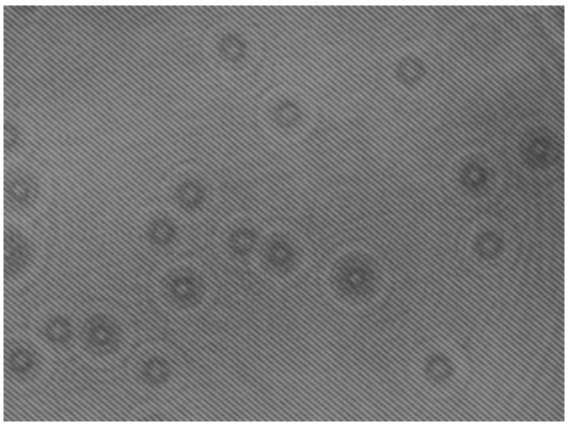

Fig.3.2. Diffraction pattern of the small particles

3.2. Reconstruction of digital holograms

In digital holography, the superposition of the object wave and reference wave produces a holographic interference pattern that is recorded by a CCD camera. Using the ASM, one can extract information about the wave field that gives rise to the holographic interference pattern [3.7]. Suppose that the hologram plane and the parallel image plane are designated by the (x,y,z) and (x',y',z') coordinates, respectively. The two-dimensional (2D) complex wave field $u_z(x',y')$ on the parallel image plane is numerically reconstructed from the complex hologram wave field $u_o(x,y)$ using the ASM, which can accurately reconstruct the complex wave field on the image plane. The angular spectrum is the Fourier transform of the complex hologram wave field:

$$F(k_x, k_y; 0) = \iint_{-\infty}^{+\infty} u_o(x,y)\exp[-i(k_x.x + k_y.y)]dxdy \tag{3.1}$$

where k_x and k_y are the spatial frequencies. Normally, this spectrum contains the zero-order diffraction and a pair of twin-image components. The real image and virtual image are located symmetrically opposite with respect to the center of the image. The distance from each image to the center depends on the incidence angle of the reference wave, which must be large enough to ensure a complete separation of the zero-order diffraction. The zero-order diffraction and one of the twin image components can be removed by using a numerical band pass filter [3.3], and the reconstructed wave field can be obtained from the inverse Fourier transform of the filtered angular spectrum:

$$u_z(x',y';z) = \iint_{-\infty}^{+\infty} F(k_x,k_y)\exp[i(k_x.x + k_y.y + k_z.z)]dk_x dk_y \qquad (3.2)$$
$$= F^{-1}[F(k_x,k_y;0).\exp(ik_z z)]$$

where $k_z = (k^2 - k_x^2 + k_y^2)$, $k = 2\pi/\lambda$ and $'z'$ is the separation between the image plane and hologram plane. The main advantages of the ASM are consistent pixel resolution, easy filtering of noise and background components, and the possibility of small object-to-hologram distances because the minimum distance requirement does not apply. The computational procedure is no heavier in this case than for the Fresnel approximation or other methods. The numerical diffraction of the hologram results in a reconstructed optical field as a matrix of complex numbers, yielding the amplitude and phase images. One of the advantages of the system presented here is that it does not require physical scanning, as is the case for optical scanning holography. Therefore, the apparatus is not complicated to setup. Despite its simplicity, the digital holographic method offers an excellent potential for 3D microscopy in biomedical imaging applications.

3.3. Experiment and results

A schematic of the holographic system based on a Mach-Zender interferometer is shown in Fig. 3.1. It consists of two mirrors (M1 and M2) and two beam splitters (BS1 and BS2) that form the Mach–Zender interferometer. The laser beam generated by the He-Ne laser is split into two beams (reference and object beams). All the specimens are illuminated with a collimated He-Ne laser beam with a wavelength 632.8 nm. The off-axis geometry is considered, and the separation of the real image and

virtual image can be control by a second beam splitter(BS2). The holograms formed by the interference between the object and the reference beams were captured by a CCD camera with a pixel size $N_x \times N_y$=960× 960 and a pixel pitch of 4.65 μm, and were digitalized by means of a frame grabber.

We obtained the complex hologram of a 3D object of small particles varying in size from 20 μm to 30 μm that were produced by spraying liquid onto a glass slide. The diffraction pattern of small particles is shown in Fig.3.2. In Fig.3.4, we show an example of particle field digital holography and of its sectional image reconstruction. The images shown in Fig.3.4 are reconstructed amplitude images and their 3D prospective at different planes. However, we can clearly recognize the difference between Fig.4.3(a), (b) and (c) which are reconstructed at the co-ordinates z=10 mm, 21.2mm, and 51.7 mm respectively.

In reconstructing any given plane, the hologram can be viewed as containing defocused light and many spurious structures from other sections. With this method, we can choose a section containing only the focused parts of the image and their 3D display. In this way, we can visualize all the particles that are in focus in a plane if we choose an appropriate plane for reconstruction of the images. Figure 4.3(a) shows an out-of-focus plane, so the 3D perspective is insufficient for analysis. Figure 4.3(b) shows an in-focus plane that contains all the particles and its 3D perspective is sufficient for analysis. In Fig.4.3 (c) the shades of the particles are focused, and on the other hand, the diameter of the particles can be determined using this image. Therefore, only in-focus planes that contain all the particles show appropriate 3D perspectives.

We also obtained the complex hologram of a biological specimen object consisting of slide of bacteria (Candida Albican) of size about 10 μm~15 μm. The reconstructed images of bacteria and its three-dimensional prospective are shown in the Fig.3(a) and (b).

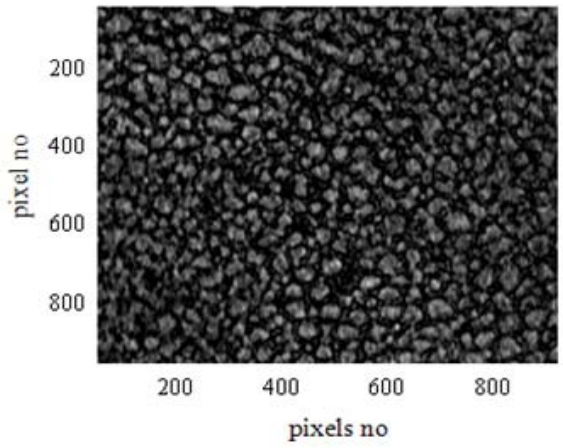

(a) Reconstructed amplitude image

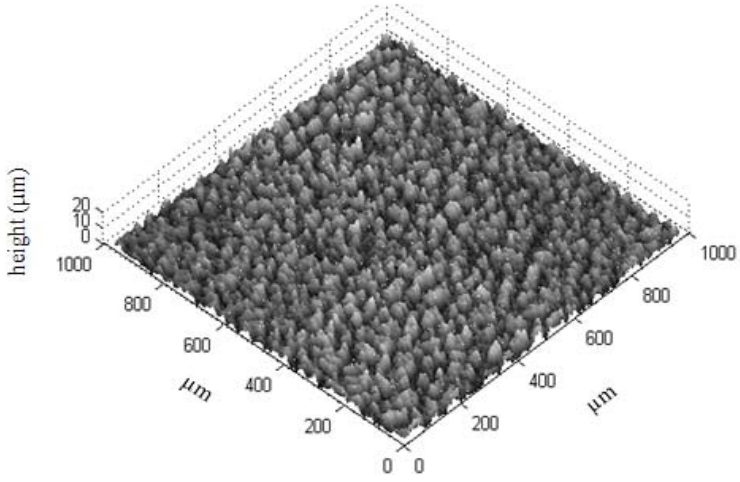

(b) 3D Prospective

Fig.3.3 Reconstructed amplitude images of bacteria at Z = 42 mm and its 3D display

(a)

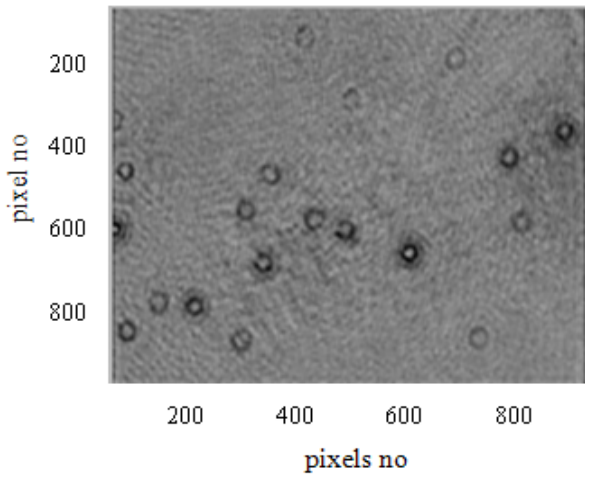
200
400
600
800
pixel no
200
400
600
800
pixels no

(b)

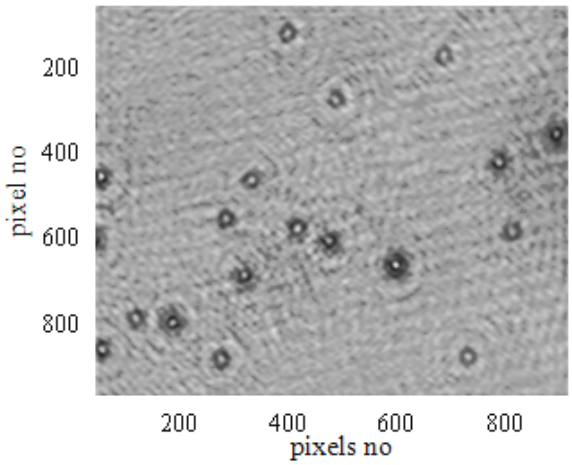
200
400
600
800
pixel no
200
400
600
800
pixels no

(c)

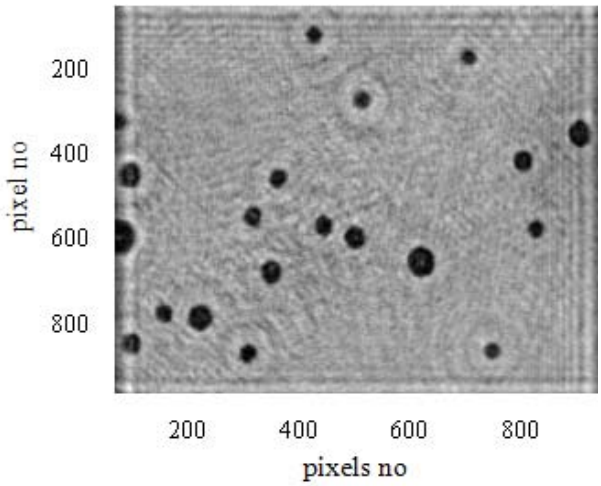
200
400
600
800
pixel no
200
400
600
800
pixels no

(d)

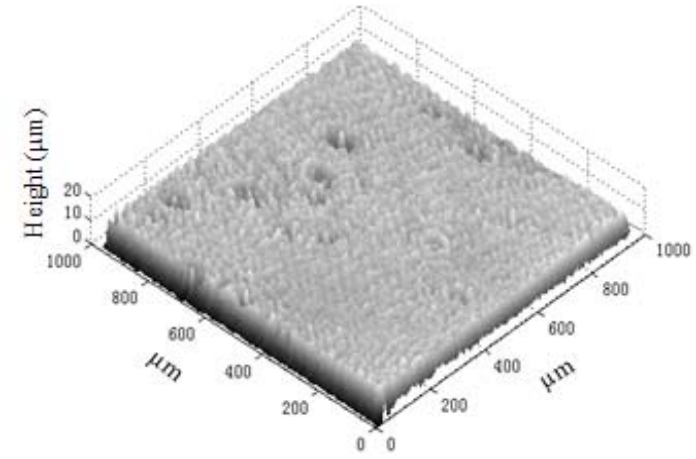

(e)

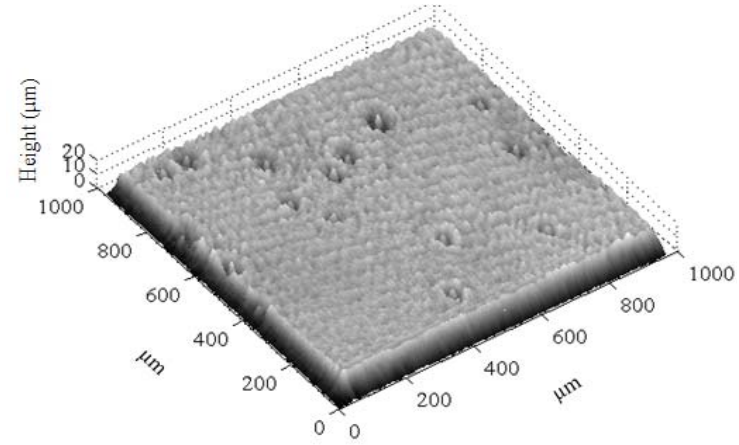

(f)

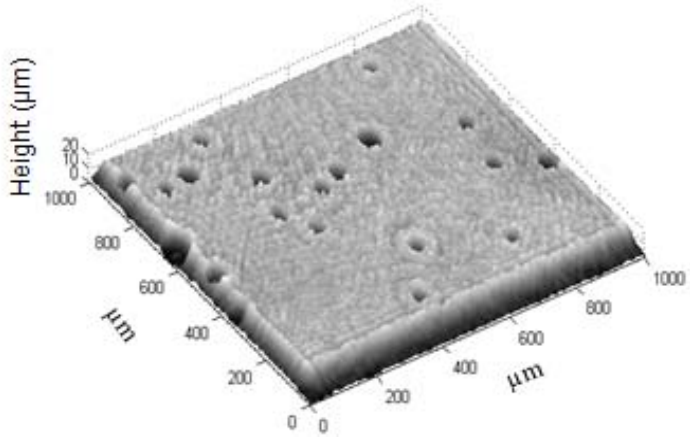

Fig.3.4 Reconstructed amplitude images at (a) Z =10mm (b) Z= 21.2 mm and (c) 51.7 mm and its 3D display are (d), (e), and (f) respectively

3.4. Discussion

In conclusion, for applications of digital holography, especially in the field of micro-measurements, studies on imaging performance are of particular importance. One of the advantages of the system presented here is that it does not require physical scanning, as in the case for optical scanning holography. Therefore, the apparatus is not complicated to setup. Despite its simplicity, the digital holographic method offers an excellent potential for 3D microscopy in biomedical imaging applications. We used holographic methods to obtain 2D and 3D images of small particles. Furthermore, a single hologram is sufficient to obtain a section containing only the focused parts of the reconstructed image. One can obtain images of different plane sections of a specimen in addition to its 3D display.

4. Reconstruction of digital hologram of small particles on arbitrarily tilted plane using digital holography

In this section, the off-axis digital holographic geometry is presented for the reconstruction of the digital hologram of small particles in an arbitrarily tilted plane. A single hologram is sufficient to obtain a well focused clear image on the tilted plane. We can't obtain clear images of small particles in the case of plane tilted to the detector plane by ordinary reconstruction method because of the rotation of the hologram plane. Rotational transformation based on coordinate rotation in Fourier space makes it possible to reconstruct holographic images in any plane in the object space. The reconstruction of digital hologram is based on the plane wave expansion of the diffracted wave-fields, using Fourier optics. With this method, the object-to-hologram distance can be quite small because the minimum distance requirement does not apply.

4.1. Introduction

Digital holography appears to be a strong contender as the next-generation technology for holographic diagnostics of particle fields, holographic particle image velocimetry for flow field measurement and three-dimensional microscopy in biomedical imaging applications [4.1-4.4]. Now, three-dimensional digital holographic microscopy has become a subject of increasing interest for many researchers. MEMS have let digital holography to gain more popularity as an effective mean of 3D microscopy [4.5-4.6].

Another superiority of digital holography is that focusing can be adjusted numerically to reconstruct images at arbitrary positions after unfocused holograms are acquired.

We can reconstruct holographic images in planes parallel to the CCD camera by ordinary techniques but one can not obtain clear images in the case of plane tilted to the CCD sensor by ordinary reconstruction method because of the rotation of the hologram plane. Reconstruction of digital holograms of small particles in tilted planes, other than the parallel planes, would be more interesting, and the reconstruction of the images on the tilted planes requires more careful consideration. Several articles explain the reconstruction of hologram on tilted planes using digital holography [4.7-4.10]. Recently, Lebrun et-al [4.11] used digital holographic method to reconstruct the small particles field in arbitrary tilted planes. This method is not sufficient for the reconstruction of the images in arbitrarily tilted planes but our method has advantages over this method for the small particles field measurement in any planes in the object space.

In this paper, the reconstruction of digital hologram is based on the plane wave expansion of the diffracted wave-fields, using Fourier optics and the two axis rotation of the wave vectors. Rotational transformation makes it possible to reconstruct holographic images on tilted plane rather than parallel one. Therefore, the transformation matrix is used to retrieve the original image. A single hologram is sufficient to obtain a well focused clear image on the tilted plane. The object to hologram distance can be any small distance without being limited by the minimum distance requirement.

Furthermore, the aim of this publication is not to present a novel

reconstruction method but to demonstrate that the selective numerical reconstruction in tilted planes may be helpful in tomographic imaging. First, the method used for reconstruction of holograms is presented, then, in the next following section, we present an experimental for small particles field reconstruction. The brief theoretical and experimental procedures are explained in the following sections.

4.2. Review of the reconstruction method

It is important to choose the appropriate reconstruction method for better image quality and high accuracy. There are many methods of numerical image reconstruction in digital holography; the main ones are Fresnel transform method, Convolution method, and Angular spectrum method (ASM) [4.12-4.15], in the order of long to short reconstruction distance. For the present work, we used the angular spectrum method to extract the information about the wave field that gives rise to the holographic interference pattern. The angular spectrum method (ASM), also known as plane wave expansion method, can accurately reconstruct the complex wave field on the image plane. Normally, in this method, we obtain Fourier transform of the diffraction pattern image, this spectrum contains the zero-order diffraction and a pair of twin-image components. The real image and twin image are located symmetrically opposite with respect to the center of the image. The distance from each image to the center depends on the incidence angle of the reference wave, which must be large enough to ensure a complete separation of the zero-order diffraction. The zero-order diffraction and one of the twin image components can be removed by using

a numerical bandpass filter [4.15], and the reconstructed wave field can be obtained from the inverse Fourier transform of the filtered angular spectrum. The main advantages of the ASM are consistent pixel resolution, easy filtering of noise and background components, and the object-to-hologram distances can be any small distance without being limited by the minimum distance requirement.

Now, we briefly describe how the complex wave field on the image plane parallel to the hologram plane is reconstructed by ASM. The coordinate systems, for the image reconstruction from a hologram, are defined as shown in the fig.4.1 where the hologram plane and the parallel image plane are designated by (x,y,z) and (x',y',z') coordinates, respectively. (X,Y,Z) set of co-ordinates are referred as tilted planes coordinate in which a wave-filed is reconstructed. Both system (image plane and titled plane) share the same origin and are not parallel to each other. The complex hologram and image wave fields $u_o(x,y)$ and $u_z(x,y)$ are considered to be the superposition of the plane waves with wave vectors $k=(k_x,k_y,k_z)$ and $k'=(k_{x'},k_{y'},k_{z'})$. Suppose their Fourier transforms are

$$U_o(k_x,k_y)=\iint_{-\infty}^{+\infty}u_o(x,y)\exp[i(k_x.x+k_y.y)]dxdy \tag{4.1}$$

$$U_z(k_{x'},k_{y'})=\iint_{-\infty}^{+\infty}u_o(x',y')\exp[i(k_{x'}.x'+k_{y'}.y')]dx'dy' \tag{4.2}$$

If $k_x=k_{x'}$ and $k_y=k_{y'}$, the only difference between $U_o(k_x,k_y)$ and $U_z(k_{x'},k_{y'})$ is the transfer function '$P(k_z)$' where 'z' is the separation between the xy-plane and $x'y'$-plane.

$$U_z(k_{x'},k_{y'})=U_o(k_x,k_y)P(k_z) \tag{4.3}$$

$$\text{where } P(k_z)=\exp(ik_z z),\quad k_z=(k^2-k_x^2+k_y^2)\ \text{ and } k=2\pi/\lambda \tag{4.4}$$

Therefore, the reconstructed wave field $u_z(x', y')$ can be obtained from the inverse Fourier transform of the complex weight $U_z(k_{x'}, k_{y'})$:

$$u_z(x', y') = F^{-1}[U_z(k_{x'}, k_{y'})] = F^{-1}[U_o(k_x, k_y).P_z(k_z)] \tag{4.5}$$

Next, the two axis rotation scheme of the method in reference [4.2] is reviewed. The components of the wave vectors of a plane wave recorded on the hologram change on the rotated image plane according to the coordinate transformation between the (x', y', z') to (X, Y, Z) spaces, shown in the fig.4.1, as follows

$$[\text{object plane}] \xrightarrow{R_{z'}(\Phi)} (x', y', z') \xrightarrow{R_{y'}(\theta)} (X, Y, Z)$$

where $R_{z'}(\Phi)=\begin{bmatrix}\cos\Phi & \sin\Phi & 0\\ -\sin\Phi & \cos\Phi & 0\\ 0 & 0 & 1\end{bmatrix}$ and $R_{y'}(\theta)=\begin{bmatrix}\cos\theta & 0 & -\sin\theta\\ 0 & 1 & 0\\ \sin\theta & 0 & \cos\theta\end{bmatrix}$.

Therefore, the wave vectors for the tilted planes one can write as

$$\begin{aligned} k_x &= k_{x'}\cos\Phi\cos\theta + k_{y'}\sin\Phi\cos\theta - k_{z'}\sin\theta \\ k_y &= -k_{x'}\sin\Phi + k_{y'}\cos\Phi \\ k_z &= k_{x'}\cos\Phi\sin\theta + k_{y'}\sin\Phi\sin\theta + k_{z'}\cos\theta \end{aligned} \tag{4.6}$$

The complex weight corresponding to the plane wave in the tilted (X, Y, Z) co-ordinate system can be obtained from the following equation:

$$\begin{aligned} &U_z(k_X, k_Y)_{tilted} \\ &= U_z(k_{x'}\cos\Phi\cos\theta + k_{y'}\sin\Phi\cos\theta - k_{z'}\sin\theta, -k_{x'}\sin\Phi + k_{y'}\cos\Phi) \end{aligned} \tag{4.7}$$

Actually there is one more factor should be considered, because $[u_z(X, Y)_{\text{tilted}}]$ is obtained from the hologram whose plane is parallel to the CCD plane but tilted relative to the y-axis. If the transformation takes place from one plane to other about the same origin, the change of the effective area should be accounted. Therefore we have to introduce an inclination factor which plays the same role as the Jacobian of the coordinate transformation [4.16]. The right hand side of the equation (7) should be multiplied by inclination factor:

$$\begin{aligned}\text{Inclination factor}(I) &= \left|\frac{\vec{i_Z}.\vec{k}}{\vec{i_Z}.\vec{k}}\right|^{1/2} = \left|\frac{k_Z}{k_{Z'}}\right|^{1/2} \\ &= \left|(k_{x'}\cos\Phi\sin\theta + k_{y'}\sin\Phi\sin\theta + k_{z'}\cos\theta)/k_{Z'}\right|^{1/2}\end{aligned} \tag{4.8}$$

where $\vec{i_{z'}}$ and $\vec{i_z}$ are the unit vectors along the positive z' and Z axes, respectively. If the tilted angle (θ) is small, then the contribution of the Jacobian or inclination factor is negligible, but in the case of large angle, Jacobian of the coordinate transformation or inclination factor becomes more important and need very careful consideration. In the case of the small particles field, its contribution to the reconstructed image is negligible except for the uniform change in the brightness of the image. The complex wave-filed $[u_z(X, Y)_{tilted}]$ on the tilted plane can be obtained from the inverse Fourier transformation of $U_z(k_{x'}, k_{y'})_{tilted}$ as follows;

$$\begin{aligned}u_z(X, Y)_{tilted} &= F^{-1}[R_{y'}[R_{z'}[F(u_o(x, y)).p_z(k_z)]]] \\ &= F^{-1}[R_{y'}[R_{z'}[U_o(k_x, k_y).p_z(k_z)]]] \\ &= F^{-1}[R_{y'}[R_{z'}[U_z(k_{x'}, k_{y'})]]] \\ &= F^{-1}[U_z(k_{X'}, k_{Y'})_{tilted}]\end{aligned} \tag{4.9}$$

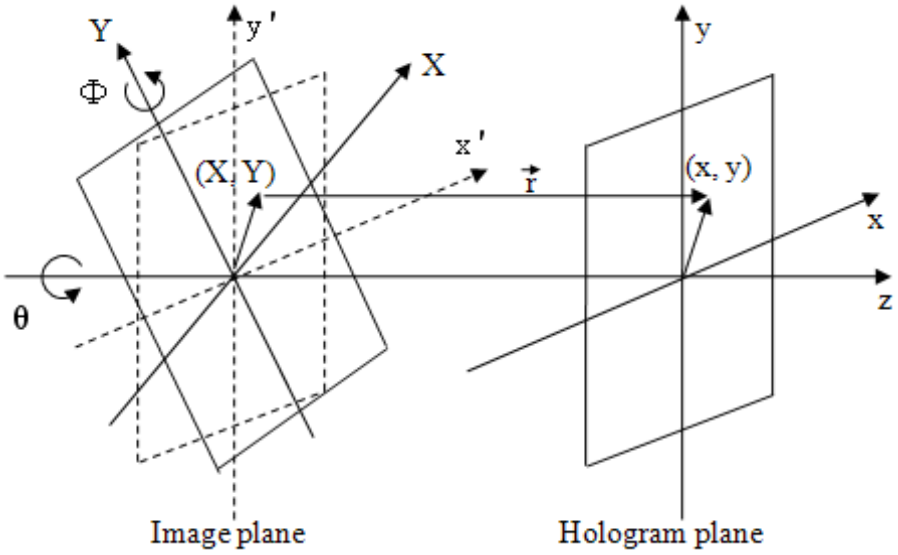

Fig.4.1.Geometrical configuration of the image and the hologram planes

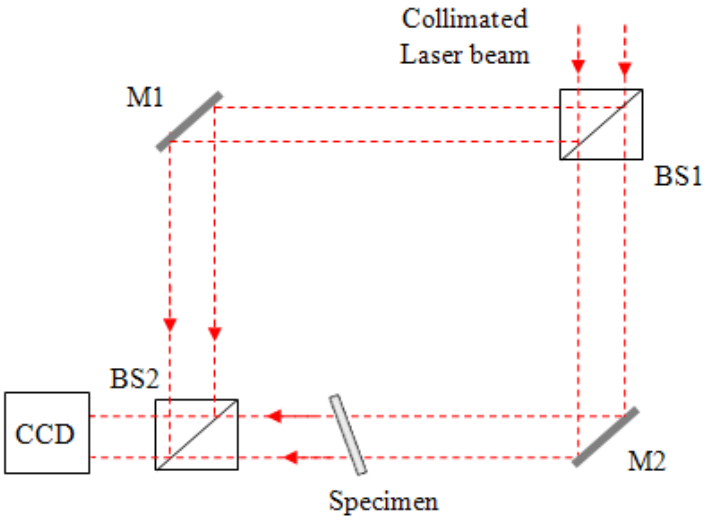

Fig.4.2.Set-up of the digital holographic system, BS, BS, beam splitters; M1, M2,mirrors;

4.3. Experiment and results

Reconstruction of digital holograms on the tilted planes requires more careful consideration. As rotational transformation is useful for wave optics, especially for digital holography, its formulation and usefulness were verified by demonstrating that images in tilted planes can be clearly reconstructed from the wave field captured by digital holography. This method leads to significant results when applied to a particle field. The schematic of two-axis rotation is shown in Fig.4.1. The image plane is purely rotated if we make the rotation only about z-axis, which is not an interesting case, because the image plane still parallel to the hologram plane and for small particles only position of the particles on the image plane changes. In this case we can reconstruct holographic images by ordinary techniques.

A schematic of the holographic system based on a Mach-Zender interferometer is shown in Fig.4.2. It consists of two mirrors (M1 and M2) and two beam splitters (BS1 and BS2) that form the Mach–Zender interferometer. The specimen was illuminated with a collimated He-Ne laser beam of a wavelength 632.8 nm. The off-axis geometry is considered, and the separation of the real image and virtual image can be control by a second beam splitter (BS2). The holograms formed by the interference between the object and the reference beams were captured by a CCD camera with a pixel size $N_x \times N_y$=1280× 960, a pixel pitch of 4.65 μm and were digitalized by means of a frame grabber. For convenience, the transformations were performed after padding the 1280 × 960 original wave field with zeros to make a square matrix (1280 × 1280), so that the pixel size in the k_x direction is the same as that in the k_y direction.

We obtained the complex hologram of small particles (size: 20μm~30μm) that were produced by spraying liquid onto a glass slide. The centre of the slide glass of the small particles was located on the optical z-axis at a distance '42.8 mm' in front of the CCD plane. The diffraction pattern of the small particles on tilted plane and its Fourier transformation are shown in the Fig.4.3(a) and Fig.4.3(b) respectively. In this experiment, first the object is rotated by −45° about the z-axis and 42° about the y-axis relative to the CCD axes respectively. Therefore, the transformation matrix is used to retrieve the original pattern.

Figure 4.4(a) shows the reconstructed image in a plane parallel to CCD plane by ordinary reconstruction method. We can see that one of the particles is in focus where as the other particles are defocused because of the rotation of the image plane. Well focused image is reconstructed and shown in the Fig.4(b), by using rotation transformation. Therefore, rotational transformation should be used to obtain a clear image of the particles. This rotational transformation has the advantage of easy implementation and fast calculation because the transformation can be performed by just a double FFT and an interpolation. However, numerical reconstruction of transparent objects by using rotational transformation based on coordinate rotation in Fourier space may be interesting for biological applications.

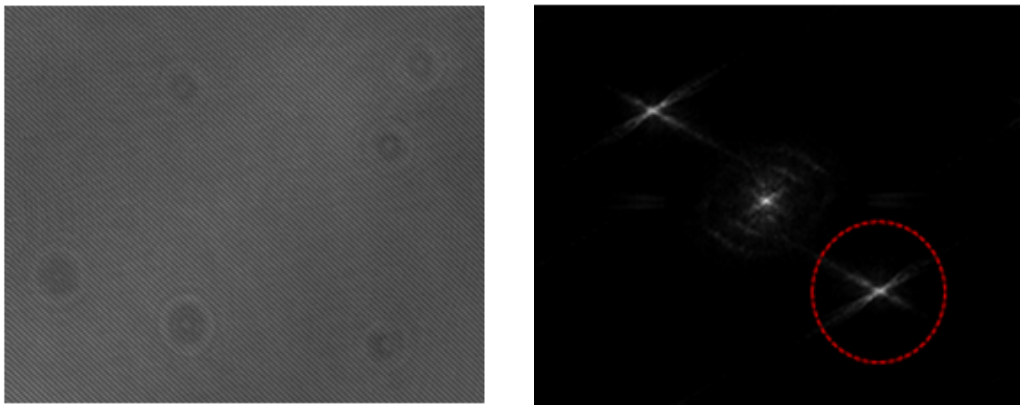

Fig.4.3 (a) Diffraction pattern (b) Fourier transform image

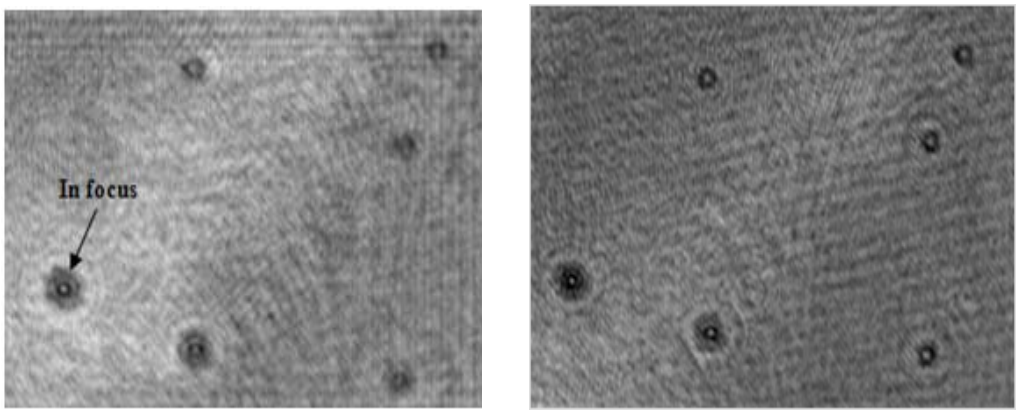

(a) parallel plane (b) tilted plane

Fig.4.4. Reconstructed amplitude images parallel to the CCD and a plane tilted to the CCD

4.4. Discussion

We can reconstruct holographic images in planes parallel to the CCD sensor by ordinary techniques but, we can't obtain clear images of small particles in the case of non-parallel plane by ordinary reconstruction method because of the rotation of the hologram plane. Rotational transformation should be used to reconstruct a clear image on the surface of the object plane and it makes possible to reconstruct tomographic images in any plane in the object space. The experimental results show that in this method it's not necessary to scan multiple planes to reconstruct images located in different object plane. One of the main advantages of the system presented here is that it does not require physical scanning, as in the case for optical scanning holography. This point is may be useful for 3D particle tracking and particularly in velocity measurements. Furthermore, a single hologram is sufficient to obtain a well focused image on the tilted plane by angular spectrum method using rotation transformation. However, the image reconstruction of transparent objects, in any plane in the object spce, may be interesting for some biological applications by this method.

5.Location of delamination in laminated composite plates by pulsed laser holography

The location of delamination in composite laminates based on their vibration characteristics is presented in this paper. Composite materials are widely used as structural materials for aerospace engineering, because of its excellent mechanical properties such as light weight, high stiffness and anti-corrosion characteristics. This paper uses pulsed electronic speckle pattern interferometry (Pulsed-ESPI) to perform non-destructive evaluation of carbon fiber reinforced plastic (CFRP) laminate plates containing various sizes of artificial defects located at the centre of the specimen, based on vibration characteristic using double-pulsed Ruby laser with a pulse duration of 30 ns. The pulsed separation can be adjusted in between 2 and 800 μs. The main advantage of this technique over conventional ESPI is the ability to carry out measurements even under harsh environmental conditions. From the results, it seems to be effective for the detection of defects in various kinds of composite materials. In this paper, the basic principles of the technique are described briefly.

5.1. Introduction

Carbon Fiber Reinforced Plastics (CFRP) is one of the advanced composite materials, widely used in various areas, especially in the space and aviation industries where they are subjected to dynamic loads. The typical structures made of CFRP laminates are subscribable to out-of-plane impact damages, such as delamination or crack-like damages between interfaces, since there

are no reinforcements through the thickness of the laminates. Delamination is one of the most common and dangerous damages, caused by internal failure of the laminas interface. It significantly reduces the strenghth and stifnes of CFRP structures. Various non destructive testing (NDT) methods have been proposed and developed for assessing internal damages in composite structures [5.1-5.3].

Electronic speckle pattern interferometry (ESPI), which was first proposed by Butters and Leendertz [5.4] to investigate the out of plane vibration behavior, is a kind of laser speckle interferometry with the advantages of non-destructive, non-contact, high resolution and real-time measurement technique of deformation for structures subjected to the various kind of loadings. Holographic interferometry has opened a new area of research making possible accurate measurement of small dynamic surface displacements for wide variety of objects [5.5-5.7].

Different methods of holographic interferometry have been developed for vibration analysis. Pulsed holography has been widely used for some time to analysis of dynamic problems. The main advantage of this technique over conventional ESPI was the ability to carry out measurements even under harsh environmental conditions.

This paper uses pulsed electronic speckle pattern interferometry (Pulsed-ESPI) to perform non-destructive evaluation of carbon fiber reinforced plastic (CFRP) laminate plates containing various sizes of artificial defects located in the centre of the specimen, based on vibration characteristic using double-pulsed Ruby laser with pulse duration of 30 ns. The pulsed separation can be adjustable in between 2 and 800 μs. The basic

principles of the technique are described briefly.

5.2. Principle of one-dimensional (1D)-Pulse ESPI

Pulse ESPI has been widely used for analysis of vibration and the dynamic behavior of the structures. It has already been presented as a non contact and full field measuring technique, which provides complete vibration maps of any component of the specimen during the test. Recently these techniques have not only taking over the main advantages of holography towards conventional measuring techniques, such as full field, non contact and sensitive to environment, but also uses modern video and computer techniques for image capturing and processing. These techniques are based on method that allows real time high-resolution filed measurements with no contact to the inspected object. Holographic interferometry has been used as a powerful technique in the measurement of vibration mode and surface displacement. However, the analysis of the measurement is very complicated. Following this technique, several speckle interferometry techniques were developed. There recording and reconstruction process were not fairly simple. The detector plane of the camera is located in the image plane of the speckle interferometer. Under these conditions, the output signal from the CCD camera, as obtained from the object in its initial state, is recorded in the computer memory. The object is then displaced, and the live camera signal is subtracted or added electronically from the stored signal. The area of the two images where the speckle pattern remains constant will give a resultant signal of zero, whereas the areas where the pattern changed give non-zero signals [5.8-5.10].

The set-up of the pulse ESPI system is shown in Fig-5.1. The object is illuminated by a laser. The most common choice is a Ruby pulse laser. The pulse laser typically emits very short, high-energy laser pulses with duration of approximately 30ns. In double pulse operation, two pulses of this type are emitted with an adjustable separation in the range between 2-800μs. The extremely short times and high performance makes the pulse laser an ideal tool for vibration and deformation analysis measurements. The reflected light is recorded by a CCD camera and processed by an image processing computer. The reference beam is directly coupled into the camera head via glass fiber, to enable flexible application in a variety of conditions. The laser pulses are controlled by a trigger system and can be selected according to the ideal application requirements. All recorded data are automatically analyzed by the measurement and analysis software.

5.2.1. Spatial Phase shift

The aim of the phase shift procedure is to find out the exact value and sign of the phase difference between the object beam and reference beam. For the pulse ESPI, the phase shifted images have to be taken simultaneously. This is achieved by doing the phase shift in spatial domain rather than temporal. It is possible by introducing an angle between the object beam and reference beam. Thus, a carrier frequency with a pixel period of 3 (120^o) and 4(90^o) develops, respectively. The angle between the beams is adapted in such away that an additional known phase difference (e.g., $\Delta\Phi = 120^\circ$) between one pixel and a neighboring pixel develops. Looking at a small area only several pixels of the CCD camera, the

structure of the phase shift procedure is similar to the one shown in Fig. 5.2. The wave fronts of the object beam and the reference beam have the unknown phase difference (Φ). The superimposing of two beams lead to interference and resulting intensity is given by Eq. (5.1)

$$I_{res} = I_{obj} + I_{ref} + 2\sqrt{I_{obj} I_{ref}}\cos\Phi \qquad (5.1)$$

Where I_{res} is resulting intensity, I_{obj} is intensity of object beam and I_{ref} is the intensity of reference beam, respectively. These are the three unknown quantities to be determined. One can measure the three intensities ($\mathbf{I}_1$, $\mathbf{I}_2$ and $\mathbf{I}_3$) at time t_1 at the neighboring pixels for the determination of the phase relation representing in equation (5.5).

$$I_1 = I_o[1 + \gamma\cos\Phi] \qquad (5.2)$$

$$I_2 = I_o[1 + \gamma\cos(\Phi + 120^o)] \qquad (5.3)$$

$$I_3 = I_o[1 + \gamma\cos(\Phi + 240^o)] \qquad (5.4)$$

Where γ is the fringe visibility. After solving above equation one can get the following equation,

$$\text{Phase shift}(\triangle\Phi) = \arctan\left[\sqrt{3}\,\frac{(I_3 - I_2)}{2I_1 - I_2 - I_3}\right] \qquad (5.5)$$

A plane wave front for the object beam over three and four pixels, respectively, has to be available in order to correctly calculate the phase relation. That means the speckle size should be three and four times, respectively, higher than for the temporal phase shift procedure.

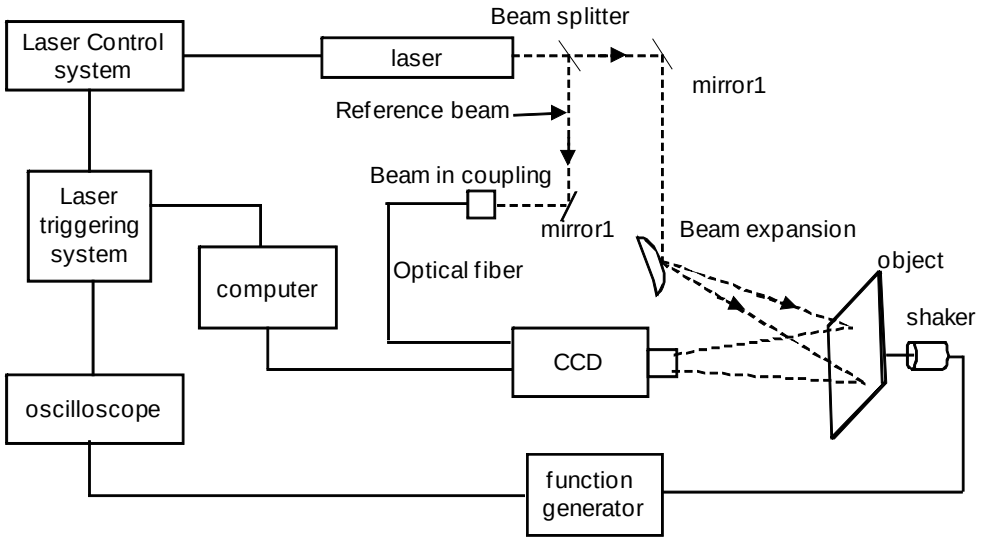

Fig.5.1 The layout of experimental set-up

5.3. Experimental set-up and specimen

The structure and shape of specimens is shown in Fig-5.3. The composite plates were made of 8 piles of uni-directional prepreg sheets of carbon fiber/epoxy (HANKUK carbon, CU125NS, 125g/m²), which is an anisotropic material. Its mechanical properties changes significantly with the changes of stacking orientation angles. The stacking orientation angles were varied in between 0° to 90° and stacked in the symmetrical manner $[+\theta/-\theta]_{4,}$ considering the coupling effect. During manufacturing by the autoclave, the hardening conditions were set up as the hardening temperature of 130^{o}C, the

hardening time of 90 minutes, and the vacuum pressure of 10^{-1}Pa. Outside from the vacuum bag, it was also compressed up to $3x10^5$ Pa. All the specimens were cut to have the length of 14 cm using a diamond cutter which does not generate residual stress.

Three specimens of composite plates with defects were used in this experiment. The test specimens were prepared with dimensions about (140mm x 140mm x 1.2mm). Three Teflon tapes (each of thickness 0.15mm) of different shapes were used in between first and second piles (i.e. first interface) of CFRP prepreg sheets. One of them was circular shape had diameter 30mm, while others were rectangular (size =15mmx30mm) and triangular (each side =30mm).

The principal set-up of a pulse ESPI system designed by Steinbichler is shown in Fig-5.1. It consists of Ruby laser system (λ= 694 nm), ESPI sensor, function generator for vibration, Image processing program. Two sides of the specimen were free and two sides attached with rubber stripe. The shaker was attached to the back side of the specimen and function generator adjusts the excitation frequency. The distinct frequency characteristic was used for the defect detection. All recorded data are automatically analyzed by the measurement and analysis software, FRAMES *plus*. The results can be displayed as color presentations, 3D graphics and many more.

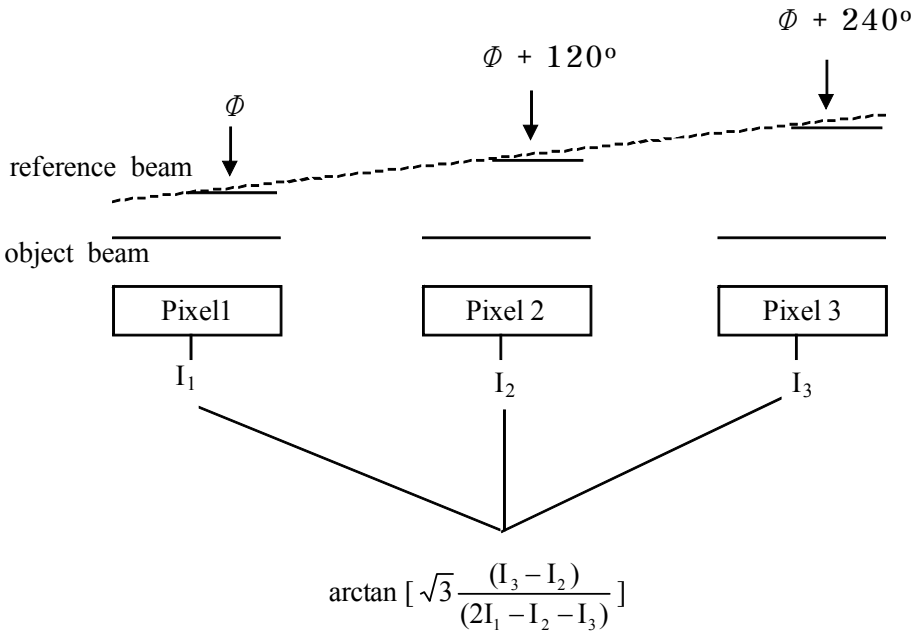

Fig.5.2 Structure of the spatial phase shift procedure

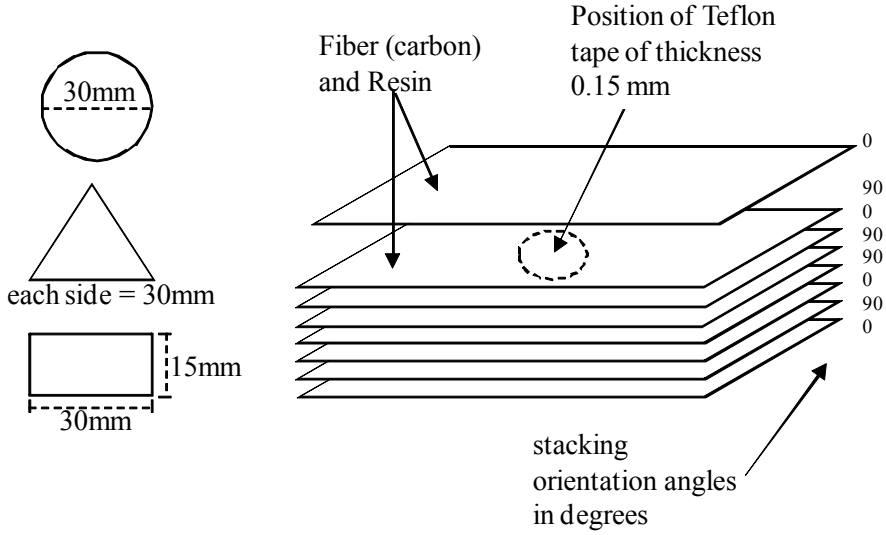

Fig.5.3. Structure of CFRP prepreg sheet with various sizes of artificial defects located at the centre of the specimen.

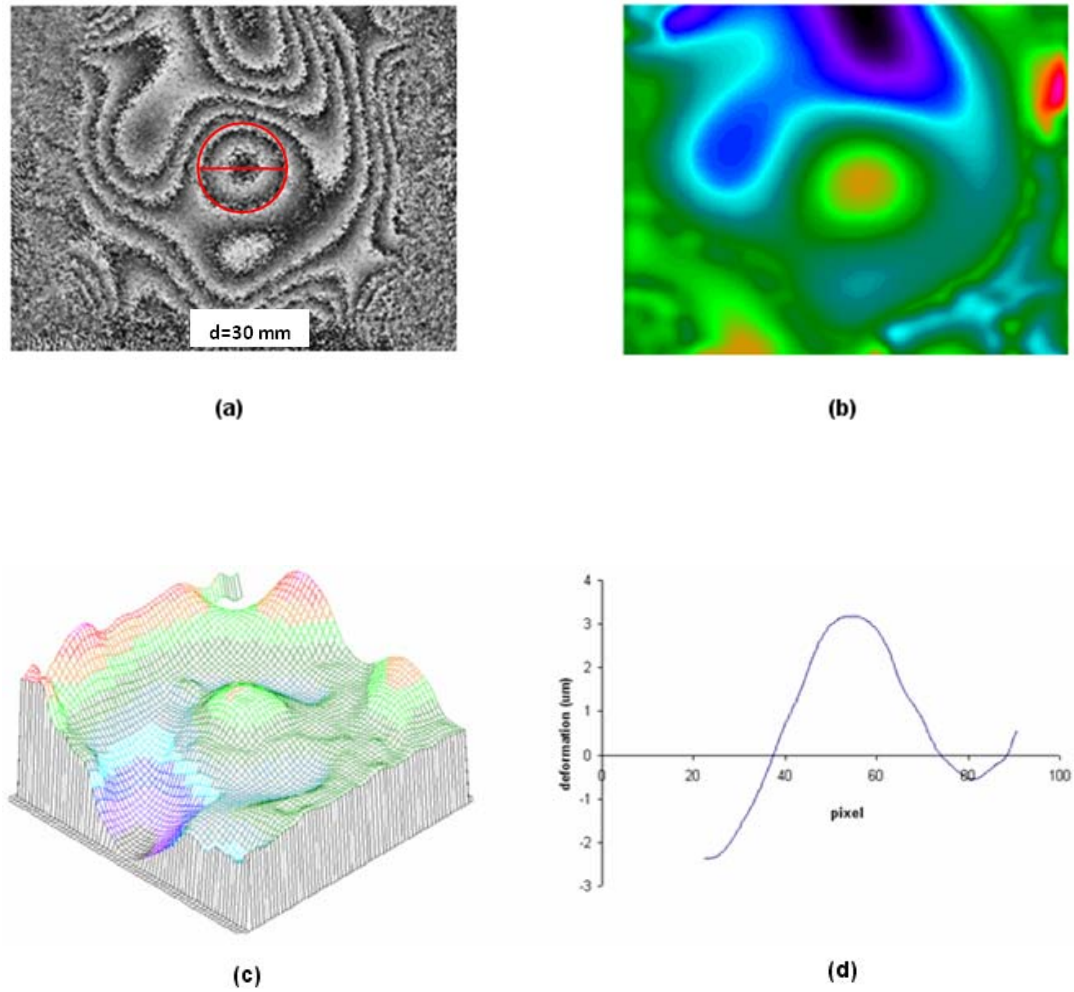

Fig.5.4 Vibration mode pattern of the laminated composite plate with circular defect at frequency 1.935 kHz (a).Phase map (b).Unwrapping Image (c). 3D Image (d) Line Profile

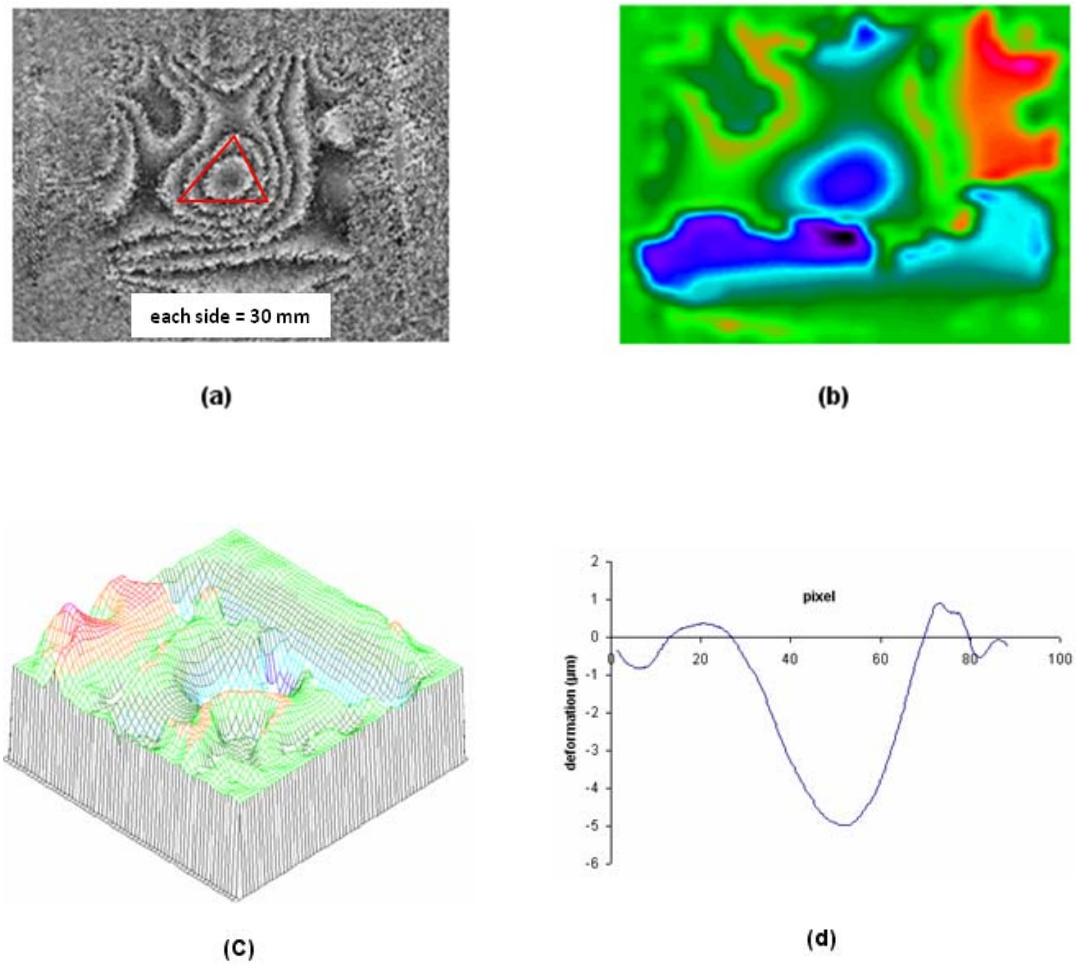

Fig.5.5 Vibration mode pattern of the laminated composite plate with triangular defect at frequency 2.157 kHz (a). Phase map (b). Unwrapping Image (c).3D Image (d) Line Profile

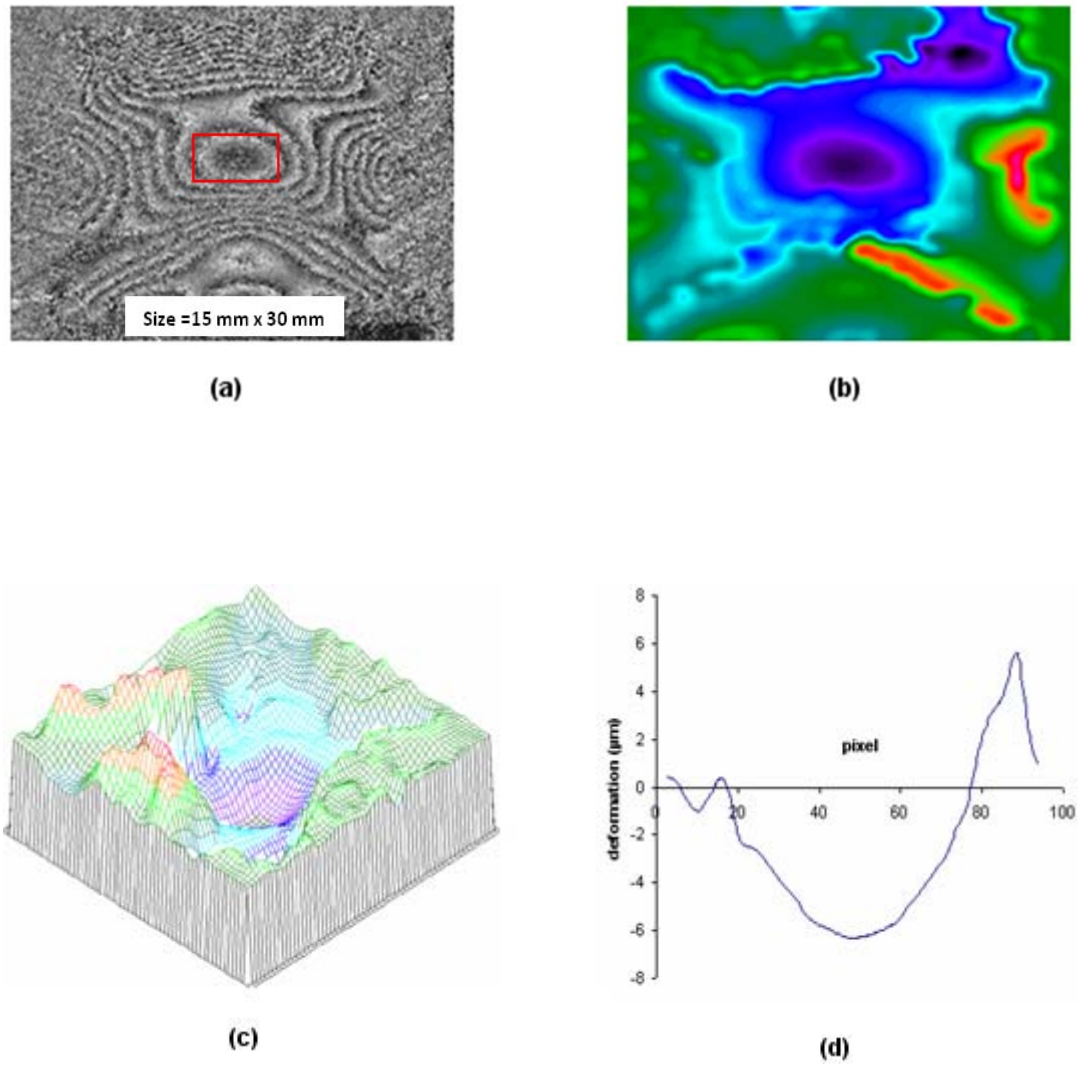

Fig.5.6 Vibration mode pattern of the laminated composite plate with rectangular defect at frequency 1.945 kHz (a) Phase map (b) Unwrapping Image (c) 3D Image (d) Line Profile

5.4. Experimental results

Images presented in Fig-5.4-5.6 represent some of the most significant results obtained in this experiment. These images were recorded by a high speed CCD camera, high power pulse laser and a fiber optics interferometer. The time delay between two pulses was 100 μ sec for all the images. The function generator adjusts the excitation frequency.

The distinct frequency characteristic was used for the delamination detection. At a certain frequency, defect part had different vibration mode shapes from the rest parts of the specimen. The circular delamination has been observed at frequency 1.935 kHz, while remaining two defects, triangular and rectangular shape observed at frequencies 2.157 kHz and 1.945 kHz respectively. Fig-5.4(a) and (b) show the phase map and unwrapping images of composite plates with circular defect. The circular fringes at the centre of the images are identified as artificial delamination. Similarly for other cases, the fringes observed at the centre of the specimen show the delaminations. Fig-5.5(a) & (b) and 5.6(a) & (b) show the phase map and unwrapping images of composite plates with triangular and rectangular delaminations respectively. For unknown cases, one can also detect the delamination after the determination of resonance frequencies of the plate.

After the observation of the images, it is possible to conclude that such kind of delamination can be easily revealed. It is quite difficult to determine the exact size of the delamination, but the specimen of different shapes of delamination has different mode shape of vibration. Therefore, it is possible to estimate the shape of the delamination, but not the exact

shape and size by this method.

5.5. Discussion

In this study, delamination in laminated composite plates was investigated experimentally using a phase shifting pulsed digital holography. The delamination in composite plates was visualized and analyzed by phase shift interferometer, with single reference beam. Furthermore, this study can be applied to defect detection in laminated composite plates and one can measure their shape and size as an NDT tools. As main advantage of pulsed digital holographic techniques we can reduce the external environmental disturbances.

6. Summary and conclusion

In the past several decades three-dimensional optical imaging has emerged as a leading tool for scientific discovery in many different fields, including materials science, condensed matter physics, and biology.

In conclusion, for applications of digital holography, especially in the field of micro-measurements, studies on imaging performance are of particular importance. One of the advantages of the system presented here is that it does not require physical scanning, despite its simplicity, the digital holographic method offers an excellent potential for 3D microscopy in biomedical imaging applications.

We can reconstruct holographic images in planes parallel to the CCD sensor by ordinary techniques but, we can't obtain clear images in the case of plane tilted to the CCD sensor by ordinary reconstruction method because of the rotation of the hologram plane. Rotational transformation should be used to reconstruct a clear image on the surface of the object plane and it makes possible to reconstruct tomographic images in any plane in the object space. Furthermore, a single hologram is sufficient to obtain a section containing only the focused parts of the reconstructed image.

Non-destructive applications of laser holography is used to locate the delamination in laminated composite palates by pulsed laser holography. Furthermore, this study can be applied to defect detection in laminated composite plates and one can measure their shape and size as an NDT tools. As main advantage of pulsed-Laser digital holographic techniques is that one can reduce the external environmental disturbances. From the results, it seems to be effective for the detection of defects in various kinds

of composite materials.

There are still some challenges to using holography as a general-purpose 3D imaging technique. Today, with fast Fourier transform algorithms, we can reconstruct a hologram for a single z-section within a few tenths of a second on a common PC. But we generally work with thousands of holograms taken at different times, and for each hologram we reconstruct a volume consisting of about a thousand different z-sections. Some work therefore remains to be done before digital holographic method (DHM) can replace confocal microscopy as a general tool, but in the meantime there are specific systems and important scientific questions that can be probed using DHM. An intriguing possibility is biological imaging. Several studies have demonstrated that holographic microscopy can be used to image subcellular structures in three dimensions in near real time.

Holographic microscopes could offer huge reductions in cost and sample preparation time over confocal microscopy. In fact, the most expensive part of a DHM is the only computer that is used to reconstruct the images.

References

[1.1].Gabor, D., “A new microscopic principle”, Nature, 161, 77-778 (1948).

[1.2]. Leith, E. N. and Upatnieks, J., “Reconstructed wavefronts and communication theory”, J. Opt. Soc. Am. 52, 1123-1130 (1962)

[1.3]. Yamaguchi, I. and Zhang, T., “Phase-shifting digital holography,” Opt. Lett. 22, 1268–1270 (1997).

[1.4]. Zhang T. and Yamaguchi I., Three-dimensional microscopy with phase-shifting digital holography. Opt. Lett. 23 (15),1221–1223 (1998).

[1.5]. Kreis T. and Juptner W. P. O., “Suppression of the dc term in digital holography,” Opt. Eng. 36, 2357-2360 (1997).

[1.6]. Zhang Y., Lu Q., and Ge B., “Elimination of zero-order diffraction in digital off-axis holography,” Optics Communication, 240, 261-267 (2004)

[1.7]. Chen G.-L., Ching-Yang L., Ming-Kuei K., and Chi-Ching C. “Numerical suppression of zero-order image in digital holography.” OPTICS EXPRESS/ Vol. 15, No. 14, 8851-8856 (July 2007).

[1.8]. Cuche, Etienne; Marquet, Pierre; Depeursinge, Christian ,”Spatial Filtering for Zero-Order and twin-Image Elimination in Digital Off-Axis Holography. “Applied Optics, Vol. 39, Issue 23, 4070-4075 (2000).

[1.9]. Goodman J.W. and Lawrence R.W., “Digital image formation electrically detected holograms,” Appl. Phys. Lett. 11, 77-79 (1967).

[1.10]. Kronrod M.A., Merzlyakov N.S. and Yaroslavski L.P.,“reconstruction of holograms with a computer,” Sov. Phy-Tech. Phys. USA 17, 333-334 (1972).

[1.11]. Schnars and Jüptner W., “Direct recording of holograms by a CCD target and numerical reconstruction, “ App. Opt. 33, 179-181 (1994).

[2.1]. Yamaguchi I., Kato J.-i., Ohta S., and Mizuno J., “Image formation in phase-shifting digital holography and applications to microscopy,” Appl. Opt. 40, 6177–6186 (2001).

[2.2]. Klein M. V. and Furtak T. E., Optics, 2nd edition (Wiley, NewYork, 1986).

[2.3]. Xu L., Miao J., Asundi A. Properties of digital holography based on in-line configuration“, Optical Engineering Papers 39, 3214-3219 (2000).

[2.4]. Wangner C., Seebacher S., Osten W., and Juptner W., “Digital recording and numerical reconstruction of lens-less Fourier holograms in optical metrology,” Appl. Opt. 38, 4820 (1999).

[2.5] L. Yu and M. K. Kim, “Wavelength-scanning digital interference holography for tomographic three-dimensional imaging by use of the angular spectrum method,” Opt. Lett. 30, 2092–2094 (2005).

[2.6]. Kang J. W. and Hong C. K., “Phase-contrast microscopy by inline phase-shifting digital holography: shape measurement of a titanium pattern with nanometer axial resolution,” Opt. Eng. 46, 040506 (2007).

[2.7]. Neifeld M. A., “ Information, resolution, and space-bandwidth product,” Opt. Lett. 23, 1477-1479 (1998).

[2.8]. Lohmann A.W., Dorsch R. G., Mendlovic D., Zalevsky Z. and Ferreira C., Space-bandwidth product of optical signals and systems, “ J.Opt. Soc.Am. A 13, 470-473(1996).

[2.9] Lei Xu, Xiaoyuan Peng, Zhixiong Guo, Jianmin Miao, Anand Asundi. “Imaging analysis of digital holography,” Opt. Exp. Vol. 13, No. 7, 2444-4452 (2005).

[2.10]. Cho H., Woo J-K, Kim D., Shin S., Yu Y., “DC suppression in in-line digital holographic microscopes on the basis of an intensity-averaging

method using variable pixel numbers", Optics & Laser Tech. 41 (2009) 741-745.
[2.11]. Takaki Y., Kawai H., Ohz H., "Hybrid Holographic Microscopy Free of Conjugate and Zero-Order Images," Appl. Opt. 38, 4990–4996 (1999).

[3.1] Knox C., "Holographic microscopy as a technique for recording dynamic microscopic subjects, " Science 153, 989-990 (1966).
[3.2] Zhang T. and Yamaguchi I., "Three-dimensional microscopy with phase-shifting digital holography". Opt. Lett. 23 (15), 1221–1223 (1998).
[3.3] Weijuan Qu et al "Digital holographic interferometry and the angular spectrum method applied to measuring the domain inversion in ferroelectric crystal" J. Opt. A: Pure Appl. Opt. 9, 480-485 (2007).
[3.4] Yamaguchi I. and Zhang T., "Phase-shifting digital holography," Opt. Lett. 22, 1268–1270 (1997).
[3.5] Matsushima K., Schimmel H., and Wyrowski F., "Fast calculation method for optical diffraction on titled planes by use of the angular spectrum of plane waves," J. Opt. Soc. Am. A 20, 1755–1762 (2003).
[3.6] Yamaguchi I., Kato J.-i., Ohta S., and Mizuno J., "Image formation in phase-shifting digital holography and applications to microscopy", Appl. Opt. 40, 6177–6186 (2001).
[3.7] Nicola S. De, Finizio A., Pierattini G., Ferraro P., and Alfieri D., "Angular spectrum method with correction of anamorphism for numerical reconstruction of digital holograms on tilted planes," Opt. Express 13, 9935–9940 (2005).
[3.8] Rappaz B., Marquet P., Cuche E., Emery Y., Depeursinge C.,and Magistretti P. J., "Measurement of the integral refractive index and dynamic

cell morphometry of living cells with digital holographic microscopy," Opt. Express 13, 9361–9373 (2005).
[3.9] Cuche E., Bevilacqua F., and Depeursinge C., "Digital holography for quantitative phase-contrast imaging," Opt. Lett. 24, 291–293 (1999).
[3.10] Kim T., "Optical sectioning by optical scanning holography and a Wiener filter," Appl. Opt. 45, 872–879 (2006).
[3.11] Lam E. Y., Zhang X., Huy Vo, Poon T-C., and G.Indebetouw, Three-dimensional microscopy and sectional image reconstruction using optical scanning holography, Appl. Opt Vol.48, No.34, 113-119 (2009).

[4.1]. Yamaguchi I. and Zhang T., "Phase-shifting digital holography," Opt. Lett. 22, 1268–1270 (1997).
[4.2] Yamaguchi I., J.-i. Kato, Ohta S., and Mizuno J.,"Image formation in phase-shifting digital holography and applications to microscopy," Appl. Opt. 40, 6177–6186 (2001).
[4.3] Murata S., Yasuda N, "Potential of digital holography in particle measurement." Optics & Laser Technology. 32, 567-574 (2000).
[4.4] Pan G. and Meng H., "Digital Holography of Particle Fields: Reconstruction by Use of Complex Amplitude," Appl. Opt. 42, 827-833 (2003).
[4.5] Cuche E., Bevilacqua F., and Depeursinge C., "Digital holography for quantitative phase-contrast imaging," Opt. Lett. 24, 291–293 (1999).
[4.6] Takaki Y. and Ohzu H., "Hybrid holographic microscopy: visualization of three-dimensional object information by use of viewing angles," Appl. Opt. 39, 5302–5308 (2000).
[4.7] Yu L., An Y., and Cai L., "Numerical reconstruction of digital holograms with variable viewing angles," Opt. Express 10, 1250–1257

(2002).
[4.8] L. Yu and M. K. Kim, “Wavelength-scanning digital interference holography for variable tomographic scanning,” Opt. Express 13, 5621–5627 (2005).
[4.9] Tommasi T. and Bianco B., "Computer-generated holograms of tilted planes by a spatial frequency approach", J. Opt. Soc. Am. A 10, 299-305, 1993.
[4.10] De Nicola S., Finizio A., Pierattini G., Ferraro P., and Alfieri D., “Angular spectrum method with correction of anamorphism for numerical reconstruction of digital holograms on tilted planes,” Opt. Express 13, 9935–9940 (2005).
[4.11] Lebrun D., Benkouider A.M., Coëtmellec S. and Malek M., “Particle field digital holographic reconstruction in arbitrary tilted planes.” Opt. Express, Vol. 11, No. 3, 224-229 (2003).
[4.12] Cuche E., Marquet P., and Depeursinge C., "Simultaneous amplitude-contrast and quantitative phasecontrast microscopy by numerical reconstruction of Fresnel off-axis holograms," Appl. Opt. 38, 6994-7001 (1999).
[4.13] Yu L. and Kim M. K., “Variable tomographic scanning with wavelength scanning digital interference holography.” Opt. Commun. 260, 462–468 (2006).
[4.14] Kim M. K., “Tomographic three-dimensional imaging of a biological specimen using wavelength-scanning digital interference holography”, Optical Express Vol. 7, No. 9 , page : 305-310 (2000).
[4.15] Weijuan Qu et al "Digital holographic interferometry and the angular spectrum method applied to measuring the domain inversion in ferroelectric crystal" J. Opt. A: Pure Appl. Opt. 9480-485(2007).

[4.16] Matsushima K., Schimmel H., and Wyrowski F., “Fast calculation method for optical diffraction on titled planes by use of the angular spectrum of plane waves,” J. Opt. Soc. Am. A 20, 1755–1762 (2003).

[5.1]. Ambu R. , Aymerich F., Ginesu F., Priolo P., Assessment of NDT interferometric techniques for impact damage detection in composite laminates. Composites Science and Technology. Papers 66, 199-205, (2006).
[5.2]. Santos F., Vaz Mario, Monteiro J., A new set-up for pulsed digital shearography applied to defect detection in composite structures. Optics and Lasers in Engineering. Papers 42, 131-140, (2004).
[5.3] Araujo dos Santos J. V., Lopes H.M.R., Vaz M., Mota Soares C.M., de Freitas M. J. M., "Damage localization in laminated composite plates using mode shapes measured by pulsed TV holography. Composite Structures. Papers 76, 272-281, (2006).
[5.4]. J. N. Butters and J. A Leendertz, Speckle pattern and holographic techniques in engineering metrology. Optics and Laser Technology. Papers 3, 26-30, (1971).
[5.5]. Labbe, F., Strain-rate measurements by electronic speckle-pattern interferometry (ESPI), Optics and Lasers in Engineering 45 (8), pp. 827-833, 2007.
[5.6]. Arai Y., Hirai H., Yokozeki S., High-resolution dynamic measurement using electronic speckle pattern interferometry based on multi-camera technology, Optics and Lasers in Engineering 46 (10), pp. 733-738, 2008.
[5.7]. Yang, L., Zhang, P., Liu, S., Samala, P.R., Su, M., Yokota, H., Measurement of strain distributions in mouse femora with 3D-digital speckle pattern interferometry, Optics and Lasers in Engineering 45 (8), pp. 843-851, 2007.

[5.8]. Cloud G. L., Optical Methods of Engineering Analysis. Cambridge University Press. (1995).

[5.9]. Rastogi P.K., and Inaudi D., Trends in Optical Non-destructive Testing and Inspection. Elsevier Science Ltd. (2000).

[5.10] Robert Jones, Holographic and speckle interferometry, 2nd ed. Cambridge University Press, Chepter 2, 1989.

ACKNOWLEDGEMENTS

First of all, I would like to thanks Almighty Lord "Allah" Most Gracious, Most Merciful, for giving me such a wonderful thing and blessed life.

It takes a long time to complete a PhD thesis. I would here like to express my thanks to the people who have been very helpful to me during the time it took me to write this thesis. I want to express my sincere thanks and gratefulness to my academic supervisor, Prof. Kyeong-Suk Kim for his advices, extreme tolerance, and patience during my PhD and for providing financial support from his research grants and giving me stability in my research career.

There were many people who gave interesting feedback and valuable suggestions for which I would like to thank them. I am highly thankful to my all seniors specially Dr. Hyun-Chul Jung, Dr. Ho-Seop Chang and Dr. Kisoo Kang for the generosity with which they helped me with statistics, and for their willingness to muse on questions I faced.

I would like to express my appreciation to all lab mates for their supports, helps, nice behaviors and good wishes. I am also thankful for the friendly behavior, cooperation and helps of my departmental colleagues and friends. Special thanks to Dong-Soo Kim, Kyung-Su Kim, and Duk-Woon Jung. I am very much impressed by the Korean people for their kindness, loving, helping nature and making life easy for foreigners. I am also thankful to all my friends whom I met during my PhD in Chosun University.

I also appreciate the advice of the committee members, Prof. Wan-Shik Jang, Prof. Jae-Yeol Kim, Prof. Dong-Pyo Hong, and Prof Man Yong Choi for their critical comments which enabled me to notice the weakness of my dissertation make the necessary improvement according to

their comments.

I shall be grateful to all my close friends around the world specially my colleagues from Aligarh Muslim University (India), during my bachelor and master course and for their cooperation, helps, many memorable events that give me fruitful memories and to learn this world.

I have been fortunate to come across many funny & good friends, without whom life would be bleak. Very special thanks to my best friend Shafiqullah for unconditional help during my visit to India with whom I shared my good and bad times. Special thanks go to Salahuddin, Sohail, Dinesh, and Zia for their ever-present support. Though it will not be enough to express my gratitude in words to all those people who helped me, I would still like to my many, many thanks to all these people.

I especially thank my parents and my family. My hard-working parents have sacrificed their lives for my brothers and sisters and provided unconditional love and care. I would not have made it this far without them. There are no words to convey how much I love them. May Almighty Allah give them a place in Jannatul Firdaus, bless them a happy, healthy and long lasting life (Aameen).

I am very lucky to have the selfless blessings, love, and caring of my family members and relatives specially my maternal uncle and aunt, I am always thankful for their love and affection towards me. I express my deepest love to my sisters, brothers and brother in laws for their endless love. Special thanks to Shams for his unconditional ever-present support and help during my visit to India.

Finally, a very special thanks to my soul-mate and wife Saba for her love and support, especially, she has been there for me through every crisis, and is an endless source of great joy and love. Your patience, love and

encouragement have upheld me, particularly in those many days in which I spent more time with my computer. No more doctorates - I promise! Saba! Now it's your turn. Special thanks to the newest additions to my family, my eight months old son "Mohammad Hammad". I am very sorry for not being present at the time of your birth. May Allah bless you a happy life and make a place for you in Jannatul Firdaus (Aameen).

I dedicate this thesis to my parents, and my family for their constant support and unconditional love. I love you all dearly.

N. Akhter
Chosun University
Gwangju, South korea

저작물 이용 허락서

학 과	기계 설계	학 번	20067754	과정	박사
성 명	한글 : 아흐터 나심		영문 : Naseem Akhter		
주 소	광주 광역시 지산동 현진빌라 168-5 102호				
연락처	e-mail : naseemalig@gmail.com				
논문제목	한글 : **디지털 홀로그램의 수치적 복원과 3차원 이미지에 대한 그 활용**				
	영문 : Numerical Reconstruction of digital holograms and its application to three-dimensional imaging				

본인이 저작한 위의 저작물에 대하여 다음과 같은 조건 아래 조선대학교가 저작물을 이용할 수 있도록 허락하고 동의합니다.

- 다 음 -

1. 저작물의 DB구축 및 인터넷을 포함한 정보통신망에의 공개를 위한 저작물의 복제, 기억장치에의 저장, 전송 등을 허락함.
2. 위의 목적을 위하여 필요한 범위 내에서의 편집과 형식상의 변경을 허락함. 다만, 저작물의 내용변경은 금지함.
3. 배포·전송된 저작물의 영리적 목적을 위한 복제, 저장, 전송 등은 금지함.
4. 저작물에 대한 이용기간은 5년으로 하고, 기간종료 3개월 이내에 별도의 의사 표시가 없을 경우에는 저작물의 이용기간을 계속 연장함.
5. 해당 저작물의 저작권을 타인에게 양도하거나 출판을 허락을 하였을 경우에는 1개월 이내에 대학에 이를 통보함.
6. 조선대학교는 저작물 이용의 허락 이후 해당 저작물로 인하여 발생하는 타인에 의한 권리 침해에 대하여 일체의 법적 책임을 지지 않음.
7. 소속 대학의 협정기관에 저작물의 제공 및 인터넷 등 정보통신망을 이용한 저작물의 전송·출력을 허락함.

동의여부 : 동의(O) 반대( )

2010 년 8 월

저작자 : Naseem Akhter (인)

조선대학교 총장 귀하